12-2021

Theoretical Development and Numerical Validation of an Asymmetric Linear Bilateral Control Model For an Automated Truck Platoon

M Sabbir Salek
Clemson University, msalek@clemson.edu

12-2021

Theoretical Development and Numerical Validation of an Asymmetric Linear Bilateral Control Model For an Automated Truck Platoon

M Sabbir Salek

THEORETICAL DEVELOPMENT AND NUMERICAL VALIDATION OF AN ASYMMETRIC LINEAR BILATERAL CONTROL MODEL FOR AN AUTOMATED TRUCK PLATOON

A Thesis
Presented to
the Graduate School of
Clemson University

In Partial Fulfillment
of the Requirements for the Degree
Master of Science
Civil Engineering

---

by
M Sabbir Salek
December 2021

Accepted by:
Dr. Mashrur Chowdhury, Committee Chair
Dr. Sakib Mahmud Khan
Dr. John Wagner

ABSTRACT

In this study, the author theoretically develops and numerically validates an asymmetric linear bilateral control model (LBCM) for an automated truck platoon, in which the motion information (i.e., position and speed) from the immediate leading truck and the immediate following truck are weighted differently. The novelty of the asymmetric LBCM is that using this model, all the follower trucks in a platoon can adjust their acceleration and deceleration to closely follow a constant desired time headway at all times to improve platoon operational efficiency while maintaining local and string stability. The author theoretically proves the local stability of the asymmetric LBCM using the condition for asymptotic stability of a linear time-invariant system and derives the condition for string stability using a space headway error attenuation approach. Then, the author evaluates the efficacy of the asymmetric LBCM by simulating a closely coupled cooperative adaptive cruise control (CACC) platoon of fully automated trucks in various non-linear acceleration and deceleration states. To evaluate the platoon operational efficiency of the asymmetric LBCM, the author compares the performance of the asymmetric LBCM to a baseline model, i.e., the symmetric LBCM, for three different time headway settings, i.e., 0.6 sec, 0.8 sec, and 1.1 sec. Analyses indicate that the asymmetric LBCM yields lower sum of squared time headway error and sum of squared speed error compared to the baseline model considered in this study. These findings demonstrate the potential of the asymmetric LBCM in improving platoon operational efficiency and stability of an automated truck platoon.

DEDICATION

I dedicate this thesis to my beloved parents and my wife for their unconditional support and motivation.

ACKNOWLEDGMENTS

I want to take the opportunity to thank all the people who were directly or indirectly involved in my journey toward this accomplishment. First, I want to convey my utmost gratitude to my advisor Dr. Mashrur Chowdhury for his constant guidance and support. Second, I am obliged to Dr. Sakib Mahmud Khan and Dr. John Wagner for their insightful comments and suggestions to improve this thesis. I want to express my gratefulness to Dr. Mizanur Rahman, Dr. Kakan Dey, and Dr. Rafiul Islam for consistently providing me with technical advice. I am also thankful to my colleagues and friends at Clemson University for providing me with motivation and mental support every time I faced a hurdle. A special thank goes to Kristin Baker for helping me out with every administrative task from my very first day as a graduate student in the Glenn Department of Civil Engineering at Clemson University. This journey toward my MS could not have been any better.

TABLE OF CONTENTS

Page

Table of Contents (Continued)

Page

LIST OF TABLES

LIST OF FIGURES

List of Figures (Continued)

Figure Page

CHAPTER ONE

INTRODUCTION

1.1 Motivation

According to the 2017 Commodity Flow Survey (CFS), US shippers used freight trucks to transport 73% of freight in terms of monetary values ("Geographic Area Series: Shipment Characteristics by Origin Geography by Mode: 2017 and 2012," 2021). Due to a mismatch between growth in freight transportation demand and surface transportation capacity, most strategic US freight corridors are characterized by varying degrees of severe congestion ("Freight and Congestion - FHWA Freight Management and Operations," 2017). The result of these recurring congestions creates stop-and-go traffic scenarios that destabilize the traffic flow and reduce freight transportation reliability. Different levels of vehicle automation, such as Adaptive Cruise Control (ACC) and Cooperative Adaptive Cruise Control (CACC) applications, allow the freight trucks to form a platoon, which improves traffic operation and reduce congestion (Arem et al., 2006; Bhoopalam et al., 2018; Kesting et al., 2008; Nowakowski et al., 2015; Ploeg et al., 2011; Tsugawa et al., 2016; Wang and Rajamani, 2002). Truck platooning improves traffic safety by automating acceleration/deceleration control and improves fuel efficiency (Tsugawa et al., 2016). As such, the trucking industry and academia have been conducting research to accelerate the mass deployment of this technology. Over the last few decades, several public-private partnerships have demonstrated automated truck platooning in real-world scenarios, most

notably the UC Berkley PATH program, which demonstrated the benefits of automated truck platooning in collaboration with the Volvo Group (Tsugawa et al., 2016).

1.2 Background

Car-following models have been used to control the longitudinal movement of automated trucks in a platoon (Martinec et al., 2014; Sugimachi et al., 2013; Zegers et al., 2017). Traditional car-following models, such as unilateral control models, use motion information only from upstream trucks and adjust their speeds depending on the leading truck's position and speed information. Thus, for a platoon under a traditional car-following model, any disturbances (e.g., sudden braking of a vehicle) within the platoon propagate only toward the upstream trucks in that platoon. This could cause traffic flow instability due to the amplification of disturbances (Horn and Wang, 2018). Some unilateral models, such as Intelligent Driver Model (IDM), have been studied in the literature to reduce the traffic flow instability in a platoon (Treiber and Kesting, 2011). However, with disturbance propagation in only upstream direction, the platoon takes time to completely absorb the disturbance.

In contrast, in a bilateral control model (BCM), this disturbance absorption can be done much more efficiently with disturbance propagation and attenuation by both upstream and downstream trucks (Horn and Wang, 2018; Wang and Horn, 2019). While the unilateral control models use only leading truck's motion information, BCMs utilize motion information from both leading and following trucks. In a platoon of fully automated trucks, getting motion information from both leading and following trucks is not an issue

as the trucks may utilize vehicle-to-vehicle (V2V) connectivity or forward and rear-facing distance and speed measuring sensors, such as radio detection and ranging (RADAR) sensors, to receive bilateral information.

Recently, Horn and Wang developed a symmetric linear BCM (referred to as the "symmetric LBCM" in the rest of this study), which can suppress traffic flow instability, especially in a stop-and-go traffic, by enabling each vehicle to adjust its speed and maintain an approximately equal distance with the immediate leading and following vehicles given they operate nearly at the same speed (Horn and Wang, 2018; Wang and Horn, 2019). Compared to other BCMs, Horn and Wang's symmetric LBCM is unique because of its capability to quickly absorb any disturbances in the traffic flow (e.g., disturbance caused by sudden braking of any vehicle in the platoon) by generating bi-directional damped waves that propagate through both upstream and downstream vehicles. However, one shortcoming of this symmetric LBCM for truck platooning application is that the symmetric LBCM does not incorporate any constant desired time headway feature in the model, which is vital for a tightly coupled platoon formation. Maintaining a small and constant desired time headway is important for truck platooning for many reasons, such as for improving platoon operational efficiency and fuel economy, and preventing vehicles from neighboring lanes to cut in (Swaroop et al., 1994; Bonnet and Fritz, 2000; Zhang and Ioannou, 2004; Bhoopalam et al., 2018).

1.3 Hypothesis and Contribution

In this study, we develop an asymmetric linear BCM (referred to as the "asymmetric LBCM" in the rest of this thesis) for truck platooning application by incorporating a constant desired time headway feature in the model. In a symmetric LBCM, motion information (such as truck positions and speeds) related to the leading and the following trucks of a subject truck are equally weighted to determine the acceleration of that subject truck, whereas our asymmetric LBCM does not use equal weights for the above case. We hypothesize that when the gap between a subject truck and its immediate leading truck is weighted more than the gap between that subject truck and its immediate following truck to determine the subject truck's acceleration, it will improve the operational efficiency of the platoon as each truck in the platoon will try to closely follow its immediate leading truck at all times. As our asymmetric LBCM is developed based on the concept of the symmetric LBCM (Horn and Wang, 2018), it inherits the unique ability of symmetric LBCM to quickly absorb any disturbances in the traffic flow by generating bi-directional damped waves that propagate through both upstream and downstream trucks. In addition, the constant desired time headway feature in the asymmetric LBCM enables the follower trucks to closely maintain a constant desired time headway in different operational states.

1.4 Objectives

The objectives of this study are as follows,

- To develop an asymmetric LBCM for longitudinal control of an automated truck platoon by incorporating constant desired time headway directly into the model,

- To theoretically analyze the local stability and the string stability of the developed model, and
- To numerically validate the platoon operational efficiency and the local and string stability of the developed model by simulating a platoon of automated trucks.

CHAPTER TWO

LITERATURE REVIEW

Different car-following models have been developed over the last several decades to model the car-following behavior of a human driver behind a leading vehicle (Gipps, 1981; Treiber et al., 2006; Chen et al., 2012; Tordeux et al., 2010; Dey et al., 2016; Sarker et al., 2020; Treiber and Kesting, 2013). These models can be broadly categorized into two classes based on the information utilization from the leading and following vehicles: (i) unilateral control models that use information from the leading vehicles only; and (ii) bilateral control models (BCMs) that use information from both leading and following vehicles. As this study focuses on developing a BCM, we review previous work related to BCMs.

Kwon and Chwa (Kwon and Chwa, 2014) developed an adaptive bi-directional platoon control model using a coupled sliding mode control method, in which each vehicle in a platoon receives information from its immediate leading and following vehicles. Although the model was able to achieve string stability, the trajectory of the follower vehicles in the platoon deviated from the leader vehicle's trajectory with non-uniform distance errors. Zegers et al. (Zegers et al., 2017) developed a multi-layer control approach for automated CACC truck platooning, in which a unidirectional CACC is responsible for information exchange in the upstream direction, i.e., from each truck to its immediate following truck, while a coordination variable is exchanged in the downstream direction, i.e., from each truck to its immediate leading truck. As a result, the subject truck is aware of the status of its following trucks and can adapt its motion accordingly. The authors

concluded that their multi-layer control approach can improve the traffic operational performance significantly in terms of a smaller spacing error. Based on bi-directional-leader following topology (i.e., only the leader vehicle has all the follower vehicles' information and the other vehicles in the platoon only receive information from their corresponding immediate leading vehicle), Li and Zhao (Li and Zhao, 2017) developed a car-following model that can capture the behavior of connected vehicles in a traffic stream. The authors evaluated the stability of their model using the perturbation method (i.e., by adding a small disturbance in the steady-state solution) and concluded that the model stability is dependent on the size of the platoon.

Recently, Horn and Wang developed a simple symmetric LBCM that can effectively suppress traffic flow instabilities and improve traffic efficiency (Horn and Wang, 2018; Wang and Horn, 2019). In the symmetric LBCM, vehicle motion information from the immediate leading and following vehicles are equally weighted. The authors showed that their model can make the traffic flow stable whereby each vehicle tries to be approximately halfway between its immediate leading and following vehicles while the platoon vehicles are operating at similar speeds. Unlike other BCMs, their symmetric LBCM incorporates a unique characteristic: a damping term is included in the model that can generate bi-directional damped waves that propagate both in the upstream and the downstream direction and quickly absorb any perturbation in the traffic flow (Horn and Wang, 2018; Wang and Horn, 2019). This unique property makes the model capable of suppressing traffic flow instability and suitable for platooning applications.

However, one major drawback of the symmetric LBCM, if it is applied for tightly coupled truck platooning applications, is that it does not directly include any desired time headway feature that can enable the follower trucks in an automated truck platoon to closely maintain a constant desired time headway at all times. Consistently maintaining a constant and small desired time headway is important for the truck platooning application as larger time headway can cause larger inter-truck gaps, which can reduce the platoon operational efficiency (as larger time headway causes reduced throughput) (Swaroop et al., 1994). A low inter-truck gap is vital in truck platooning to achieve a higher fuel efficiency by minimizing aerodynamic drag (Bonnet and Fritz, 2000) and to improve the operational efficiency of the platoon. Additionally, larger gaps can invite vehicles from neighboring lanes to cut in the middle of the truck platoon, which will affect the platoon's stability (Zhang and Ioannou, 2004). Thus, this study focuses on developing an asymmetric LBCM with the direct incorporation of a constant desired time headway feature in the model to improve the platoon operational efficiency of a closely coupled CACC platoon of fully automated trucks.

CHAPTER THREE

ASYMMETRIC LINEAR BILATERAL CONTROL MODEL

In this chapter, we present the model assumptions, model development, and theoretical analysis of local and string stability of the asymmetric LBCM, followed by a discussion about consideration of heavy-duty truck's acceleration and deceleration for the developed model.

3.1 Model Assumptions

The following assumptions are made for developing the asymmetric LBCM,

- The model is used only as a longitudinal controller for the follower trucks in an automated truck platoon,
- The platoon that uses the model is made of homogeneous trucks, i.e., all the trucks have identical lengths and vehicle dynamics,
- There are no uncertainties in the system, such as uncertainties involved in vehicle dynamics or the location and speed of neighboring trucks, and
- If the trucks utilize connectivity to exchange information, such as location and speed information then there is no delay in communication.

3.2 Model Development

As mentioned earlier, the symmetric LBCM proposed by Hong and Wang (Horn and Wang, 2018) demonstrated the capability of improving traffic flow instability in a stop-and-go traffic scenario. However, the symmetric LBCM does not include the constant

desired time headway feature into the model, which is an important parameter to form a tightly coupled platoon of trucks, in which the trucks can maintain a small, desired time headway at all times. While using the symmetric LBCM, the follower trucks will still attempt to maintain their desired time headway from their corresponding immediate leading trucks. However, for a relatively small, desired time headway, such as a time headway of 0.6 sec, not including the desired time headway directly into the control model may cause failure to maintain the desired time headway in some cases, such as following a sharp deceleration phase. Therefore, we develop an asymmetric LBCM by incorporating an additional term in the symmetric LBCM (Horn and Wang, 2018) to help maintain a constant desired time headway at all times. Equation (1) presents the linearized expression of acceleration of the asymmetric LBCM (which is also illustrated in Figure 3.1),

$$a_c = k_{d1}\left(d_l - d_f\right) + k_{d2}(d_l - d_{des}) + k_v\left[(v_l - v_c) - \left(v_c - v_f\right)\right] + k_c(v_{des} - v_c) \quad (1)$$

where, d_l is the gap (m) between a control truck (i.e., a subject truck that uses the asymmetric LBCM) and its immediate leading truck; d_f is the gap (m) between the control truck and its immediate following truck; v_l, v_c, and v_f are the speeds (m/sec) of the immediate leading truck, the control truck, and the immediate following truck, respectively; d_{des} is the desired gap (m, calculated based on the constant time headway policy as the product of a constant desired time headway ($T_{h,des}$) and v_c, i.e., $d_{des} = v_c \times T_{h,des}$); v_{des} is a desired speed (m/sec), which can be set as the speed limit of the roadway or any other desired speed that is lower than the speed limit. k_{d1}, k_{d2}, k_v, and k_c are the control gains. Here, k_{d1} and k_v are the relative distance gain and the relative speed

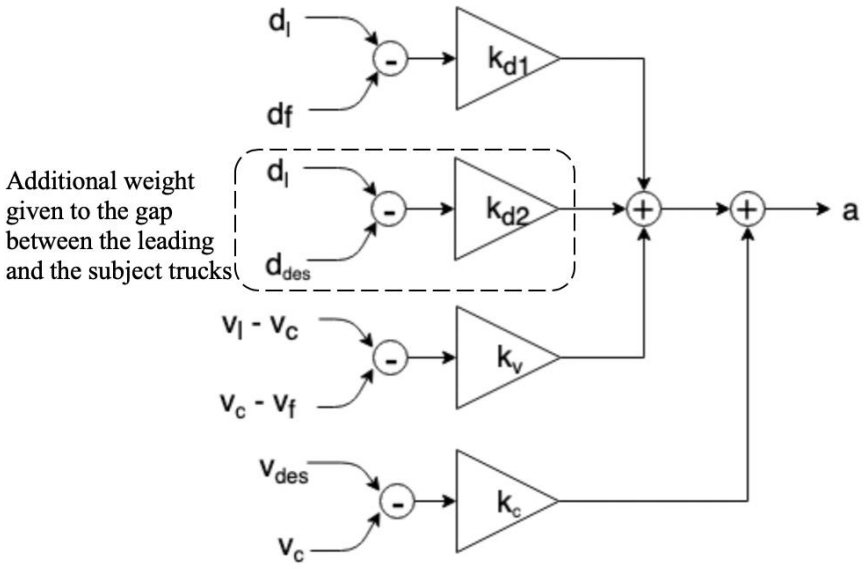

FIGURE 3.1 Illustrative diagram of the asymmetric LBCM.

gain, respectively. k_c is an optional feedback gain depending on $(v_{des} - v_c)$, i.e., the difference between the desired speed, v_{des} and the control vehicle's speed, v_c. k_{d2} represents the feedback gain depending on $(d_l - d_{des})$ or $\left(d_l - v_c T_{h,des}\right)$. In (1), $k_{d2}(d_l - d_{des})$ is the term that incorporates the constant desired time headway feature to make the platoon tightly coupled at all times.

By rearranging the right side of (1), we get,

$$a_c = (k_{d1} + k_{d2})d_l - k_{d1}d_f + k_v v_l + k_v v_f - k_{d2}d_{des} - (k_c + 2k_v)v_c + k_c v_{des} \quad (2)$$

As observed from (2), the speed of the immediate leading truck (v_l) and the speed of the immediate following truck (v_f) have the same gain (k_v). However, the gap between the immediate leading truck and the control trucks (d_l), and the gap between the control truck and the immediate following truck (d_f) have different gains, i.e., d_l is weighted

by $(k_{d1} + k_{d2})$ and d_f is weighted by k_{d1} only. This makes the model asymmetric. This additional gain (k_{d2}) comes from the term $k_{d2}(d_l - d_{des})$ that enables the model to ensure that all the automated trucks in the platoon can closely follow a constant desired time headway at all times.

In absence of a following truck, such as for the last truck in the platoon, the asymmetric LBCM reverts to a traditional cruise control or a unilateral control model, or the last truck in the platoon can invoke a virtual following truck that uses a unilateral control model, i.e., a truck can be assumed to follow the last truck of the platoon so that the last truck can also incorporate the asymmetric LBCM. The position and speed information of this virtual truck is then used by the actual last truck of the platoon.

The asymmetric LBCM is constrained by a maximum speed (v_{max}), which is set as speed limit of the roadway. The maximum speed (v_{max}) limits the acceleration of the control truck by preventing any positive acceleration when $v_c \geq v_{max}$. This prevents any unsafe operation, such as speeding over the roadway speed limit.

The asymmetric LBCM inherits the uniqueness of the symmetric LBCM of absorbing any disturbances in the traffic flow by generating a bi-directional damped wave as mentioned in (Horn and Wang, 2018) while each follower truck maintains the constant desired time headway with its immediate leading truck through the asymmetric LBCM. In (1), $k_v\left[(v_l - v_c) - \left(v_c - v_f\right)\right]$ is the damping expression that helps to absorb disturbances in the flow by generating bi-directional damped waves.

3.3 Stability of the Model

A longitudinal control model used for any automated platoon of vehicles/trucks, such as the asymmetric LBCM, must maintain local stability as well as string stability (Eyre et al., 1998; Wang and Han, 1998). In this subsection, we theoretically analyze the local and string stability of the asymmetric LBCM.

3.3.1 Local Stability

In a platoon of automated trucks, each truck can be considered locally stable if any perturbation in speed imposed by a leading truck does not cause instability, such as fluctuation in speed and/or spacing, for the follower trucks. For a BCM, speed information from both immediate leading and following trucks is used to determine the acceleration input for the control truck. Thus, exhibiting local stability for a BCM means that individual trucks should be able to maintain their own stability regardless of any perturbation imposed by their corresponding leading and/or following trucks.

In control theory, a closed-loop linear time-invariant (LTI) system, i.e., $\dot{\boldsymbol{x}} = \boldsymbol{A}\boldsymbol{x}$ is said to be asymptotically stable in the sense of Lyapunov, if and only if, all the eigenvalues of $\boldsymbol{A}$ have negative real parts (Theorem 6.3 in Williams and Lawrence, 2007). We use this eigenvalue approach to show the local asymptotic stability of the asymmetric LBCM. First, the asymmetric LBCM in (1) is written in a state-space representation using the terminology shown in Figure 3.2 as follows,

$$f_1 := \dot{x}_{i,1} = x_{i,2} \tag{3}$$

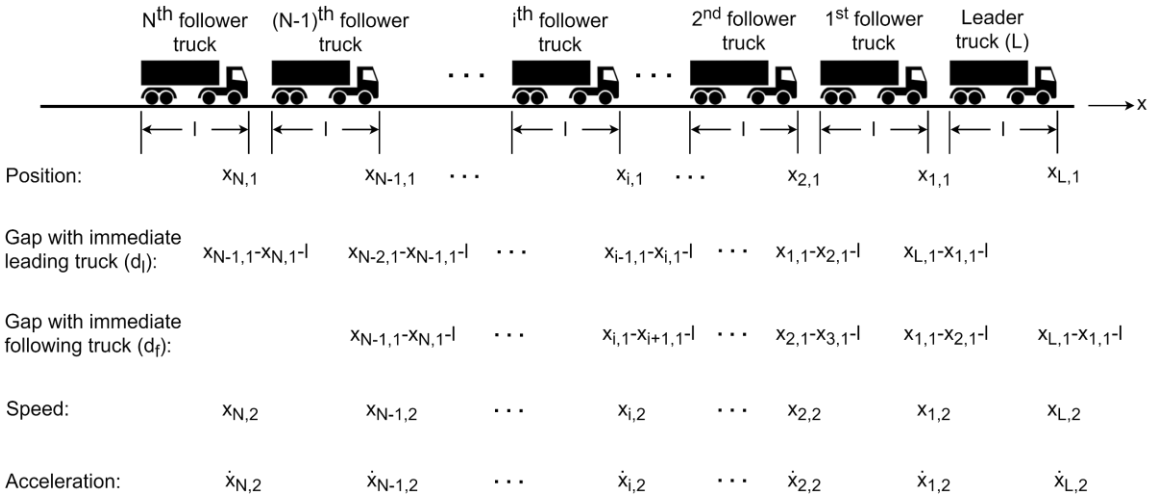

FIGURE 3.2 Terminology used in this study for a platoon of (N+1) automated trucks.

$$
\begin{aligned}
f_2 := \dot{x}_{i,2} = {} & k_{d1}\left[(x_{i-1,1} - x_{i,1} - l) - (x_{i,1} - x_{i+1,1} - l)\right] \\
& + k_{d2}\left[(x_{i-1,1} - x_{i,1} - l) - d_{des}\right] \\
& + k_v\left[(x_{i-1,2} - x_{i,2}) - (x_{i,2} - x_{i+1,2})\right] + k_c\left(v_{des} - x_{i,2}\right) \\
= {} & k_{d1}\left(x_{i-1,1} - 2x_{i,1} - x_{i+1,1}\right) + k_{d2}\left(x_{i-1,1} - x_{i,1} - l - T_{h,des}x_{i,2}\right) \\
& + k_v\left(x_{i-1,2} - 2x_{i,2} - x_{i+1,2}\right) + k_c(v_{des} - x_{i,2})
\end{aligned} \tag{4}
$$

Then, the Jacobian matrix of this system can be written as,

$$
J = \begin{bmatrix} \dfrac{\partial f_1}{\partial x_{i,1}} & \dfrac{\partial f_1}{\partial x_{i,2}} \\ \dfrac{\partial f_2}{\partial x_{i,1}} & \dfrac{\partial f_1}{\partial x_{i,2}} \end{bmatrix} = \begin{bmatrix} 0 & 1 \\ -2k_{d1} - k_{d2} & -T_{h,des}k_{d2} - 2k_v - k_c \end{bmatrix} \tag{5}
$$

The eigenvalues of the above Jacobian matrix are given by,

$$
\begin{aligned}
eig(J) = \frac{1}{2}\Bigg[& -\left(T_{h,des}k_{d2} + 2k_v + k_c\right) \\
& \pm \sqrt{\left(T_{h,des}k_{d2} + 2k_v + k_c\right)^2 - 8k_{d1} - 4k_{d2}}\Bigg]
\end{aligned} \tag{6}
$$

Careful observation of (6) reveals that $eig(J)$ will always have negative real parts $\forall k_{d1}, k_{d2}, k_v, k_c > 0$. If $\left(T_{h,des}k_{d2} + 2k_v + k_c\right)^2 \geq (8k_{d1} + 4k_{d2})$, then the eigenvalues are negative real numbers as $\sqrt{\left(T_{h,des}k_{d2} + 2k_v + k_c\right)^2 - 8k_{d1} - 4k_{d2}} < (T_{h,des}k_{d2} + 2k_v + k_c)$. On the other hand, if $\left(T_{h,des}k_{d2} + 2k_v + k_c\right)^2 < (8k_{d1} + 4k_{d2})$, then the eigenvalues are complex conjugates with the same negative real parts, i.e., $-(T_{h,des}k_{d2} + 2k_v + k_c)$. This means the LTI system described in (3) and (4) will make each truck in an automated truck platoon locally asymptotically stable in the sense of Lyapunov.

3.3.2 String Stability

For a platoon of automated trucks using any unilateral control model, string stability refers to spacing or speed error attenuation as the error propagates through the trucks in the upstream direction (Bose and Ioannou, 2001). Thus, in a BCM, attenuation should be present in both upstream and downstream directions as the error propagates in both directions. We follow the string stability analysis framework presented by Eyre et al. (Eyre et al., 1998) to derive the condition for string stability in the notion of space headway error attenuation (also known as $\mathcal{L}_\infty$ string stability) while using the asymmetric LBCM. The expression of the asymmetric LBCM presented in (1) can be rewritten in a state-space representation using the mass-spring-damper system shown in Figure 3.3 as follows,

$$\dot{x}_{L,1} = x_{L,2}$$

$$\dot{x}_{L,2} = \frac{u}{m} - \frac{k}{m}\left(x_{L,1} - x_{1,1}\right) - \frac{c}{m}\left(x_{L,2} - x_{1,2}\right)$$

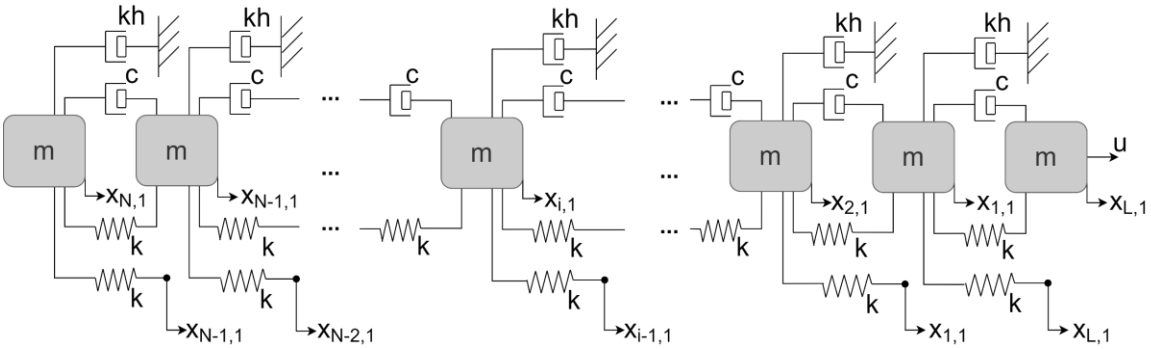

FIGURE 3.3 Mass-spring-damper system representing a platoon of (N+1) automated trucks under asymmetric LBCM.

$$\dot{x}_{1,1} = x_{1,2}$$

$$\dot{x}_{1,2} = \frac{k}{m}\left(x_{L,1} - 2x_{1,1} + x_{2,1}\right) + \frac{k}{m}\left(x_{L,1} - x_{1,1}\right) + \frac{c}{m}\left(x_{L,2} - 2x_{1,2} + x_{2,2}\right) - \frac{kT_{h,des}}{m}x_{1,2}$$

$$\dot{x}_{2,1} = x_{2,2}$$

$$\dot{x}_{2,2} = \frac{k}{m}\left(x_{1,1} - 2x_{2,1} + x_{3,1}\right) + \frac{k}{m}\left(x_{1,1} - x_{2,1}\right) + \frac{c}{m}\left(x_{1,2} - 2x_{2,2} + x_{3,2}\right) - \frac{kT_{h,des}}{m}x_{2,2}$$

$$\vdots$$

$$\dot{x}_{i,1} = x_{i,2}$$

$$\dot{x}_{i,2} = \frac{k}{m}\left(x_{i-1,1} - 2x_{i,1} + x_{i+1,1}\right) + \frac{k}{m}\left(x_{i-1,1} - x_{i,1}\right) + \frac{c}{m}\left(x_{i-1,2} - 2x_{i,2} + x_{i+1,2}\right) - \frac{kT_{h,des}}{m}x_{i,2}$$

$$\vdots$$

$$\dot{x}_{N-1,1} = x_{N-1,2}$$

$$\dot{x}_{N-1,2} = \frac{k}{m}\left(x_{N-2,1} - 2x_{N-1,1} + x_{N,1}\right) + \frac{k}{m}\left(x_{N-2,1} - x_{N-1,1}\right) + \frac{c}{m}\left(x_{N-2,2} - 2x_{N-1,2} + x_{N,2}\right) - \frac{kT_{h,des}}{m}x_{N-1,2}$$

$$\dot{x}_{N,1} = x_{N,2}$$

$$\dot{x}_{N,2} = \frac{2k}{m}\left(x_{N-1,1} - x_{N,1}\right) + \frac{2c}{m}\left(x_{N-1,2} - x_{N,2}\right) - \frac{kT_{h,des}}{m}x_{N,2} \quad (7)$$

where, $k_{d1} = k_{d2} \triangleq \frac{k}{m}$, and $k_v = \frac{c}{m}$

The above state-space representation can be transformed into space headway errors using the following transformations,

$$z_{1,1} = x_{L,1} - x_{1,1} - T_{h,des}x_{1,2}$$

$$z_{1,2} = \dot{z}_{1,1} = x_{L,2} - x_{1,2} - T_{h,des}\dot{x}_{1,2}$$

$$z_{2,1} = x_{1,1} - x_{2,1} - T_{h,des}x_{2,2}$$

$$z_{2,2} = \dot{z}_{2,1} = x_{1,2} - x_{2,2} - T_{h,des}\dot{x}_{2,2}$$

$$\vdots$$

$$z_{i,1} = x_{i,1} - x_{i+1,1} - T_{h,des}x_{i+1,2}$$

$$z_{i,2} = \dot{z}_{i,1} = x_{i,2} - x_{i+1,2} - T_{h,des}\dot{x}_{i+1,2}$$

$$\vdots$$

$$z_{N-2,1} = x_{N-2,1} - x_{N-1,1} - T_{h,des}x_{N-1,2}$$

$$z_{N-2,2} = \dot{z}_{N-2,1} = x_{N-2,2} - x_{N-1,2} - T_{h,des}\dot{x}_{N-1,2}$$

$$z_{N-1,1} = x_{N-1,1} - x_{N,1} - T_{h,des}x_{N,2}$$

$$z_{N-1,2} = \dot{z}_{N-1,1} = x_{N-1,2} - x_{N,2} - T_{h,des}\dot{x}_{N,2} \quad (8)$$

Then, the state-space representation of the space headway errors can be written as,

$$\dot{z}_{1,1} = z_{1,2}$$

$$\dot{z}_{1,2} = -\frac{3k}{m}z_{1,1} + \frac{k}{m}z_{2,1} - \frac{2c}{m}z_{1,2} + \frac{c}{m}z_{2,2} - \frac{kT_{h,des}}{m}z_{1,2}$$

$$\dot{z}_{2,1} = z_{2,2}$$

$$\dot{z}_{2,2} = \frac{2k}{m} z_{1,1} - \frac{3k}{m} z_{2,1} + \frac{k}{m} z_{3,1} + \frac{c}{m} z_{1,2} - \frac{2c}{m} z_{2,2} + \frac{c}{m} z_{3,2} - \frac{kT_{h,des}}{m} z_{2,2}$$

$$\vdots$$

$$\dot{z}_{i,1} = z_{i,2}$$

$$\dot{z}_{i,2} = \frac{2k}{m} z_{i-1,1} - \frac{3k}{m} z_{i,1} + \frac{k}{m} z_{i+1,1} + \frac{c}{m} z_{i-1,2} - \frac{2c}{m} z_{i,2} + \frac{c}{m} z_{i+1,2} - \frac{kT_{h,des}}{m} z_{i,2}$$

$$\vdots$$

$$\dot{z}_{N-2,1} = z_{N-2,2}$$

$$\dot{z}_{N-2,2} = \frac{2k}{m} z_{N-3,1} - \frac{3k}{m} z_{N-2,1} + \frac{k}{m} z_{N-1,1} + \frac{c}{m} z_{N-3,2} - \frac{2c}{m} z_{N-2,2} + \frac{c}{m} z_{N-1,2} - \frac{kT_{h,des}}{m} z_{N-2,2}$$

$$\dot{z}_{N-1,1} = z_{N-1,2}$$

$$\dot{z}_{N-1,2} = \frac{2k}{m} z_{N-2,1} - \frac{3k}{m} z_{N-1,1} + \frac{c}{m} z_{N-2,2} - \frac{2c}{m} z_{N-1,2} - \frac{kT_{h,des}}{m} z_{N-1,2} \quad (9)$$

As mentioned before, a string stable BCM helps propagate and attenuate any disturbances bidirectionally. However, the first and the last masses in a BCM are unique because they do not have any immediate leading and following masses, respectively. Thus, the string stability analysis of a bilateral control can be done unidirectionally as the first and the last masses have immediate neighbors in only one direction. As mentioned by Eyre et al. (Eyre et al., 1998), the conditions for string stability of a bilateral control can be derived by considering the last two masses in the mass-spring-damper system. The space headway error transfer function for the last two masses can be written from (9) as,

$$G(s) = \frac{z_{N-1,1}(s)}{z_{N-2,1}(s)} = \frac{\frac{c}{m}s + \frac{2k}{m}}{s^2 + \left(\frac{2c + kT_{h,des}}{m}\right)s + \frac{3k}{m}} \quad (10)$$

To ensure string stability of the asymmetric LBCM, $|G(j\omega)| < 1$, $\forall\omega > 0$. From (10), it can be shown that $|G(j\omega)| < 1$, $\forall\omega > 0$, when,

$$\frac{c}{m} > -\frac{2kT_{h,des}}{3m} + \frac{1}{3}\sqrt{\left(\frac{kT_{h,des}}{m}\right)^2 + \left(18 - 6\sqrt{5}\right)\frac{k}{m}} \tag{11}$$

which can be rewritten in terms of k_d and k_v (here, $k_{d1} = k_{d2} \triangleq k_d$) as follows,

$$k_v > \frac{1}{3}\left[-2k_d T_{h,des} + \sqrt{\left(k_d T_{h,des}\right)^2 + \left(18 - 6\sqrt{5}\right)k_d}\right] \tag{12}$$

The above inequality expression provides the condition for string stability of the asymmetric LBCM. Figure 3.4 shows the regions of string stability (indicated with upward arrows) for three different $T_{h,des}$ used in this study later for numerical validation, i.e., $T_{h,des}$ = 0.6 sec, 0.8 sec, and 1.1 sec. Thus, (12) provides constraints that can be used to tune k_d and k_v in the asymmetric LBCM. Similar constraints can be derived for the symmetric LBCM, which has been presented in Appendix A. However, the condition for string

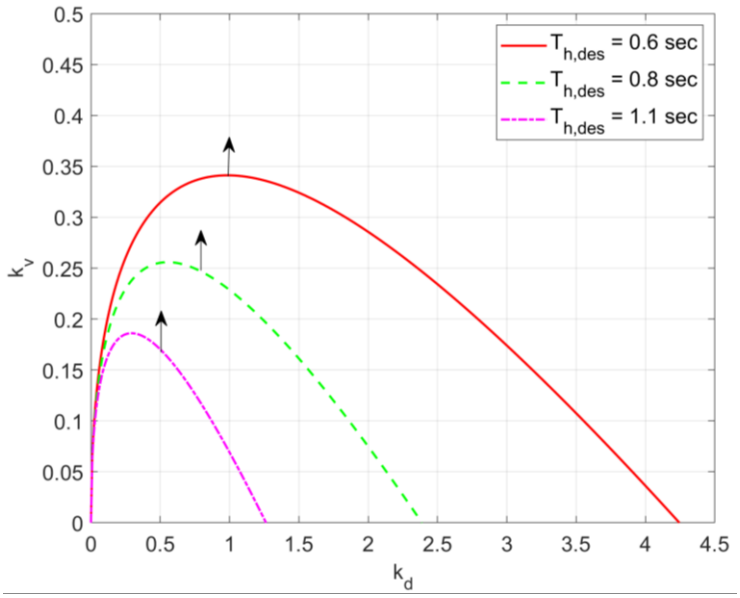

FIGURE 3.4 Regions of string stability for the asymmetric LBCM in relative speed gain (k_v) vs. relative distance gain (k_d) plane for various desired time headways ($T_{h,des}$).

stability of the symmetric LBCM does not depend on $T_{h,des}$ unlike the condition for string stability of the asymmetric LBCM because the symmetric LBCM does not directly include a constant desired time headway term as mentioned before.

3.4 Consideration of Acceleration and Deceleration Behavior of a Heavy-Duty Truck

Although the control model gives the desired acceleration at each timestamp, the maximum possible acceleration or deceleration is limited by the vehicle dynamics of heavy-duty trucks. Unlike light-weight vehicles (e.g., passenger cars), heavy-duty trucks have limited acceleration and deceleration capabilities due to their high weight-to-power ratio. To set the maximum acceleration rate for the heavy-duty trucks considered in this study (as a part of truck vehicle-dynamics consideration), we assume a 200 lb/hp weight-to-power ratio based on National Cooperative Highway Research Program (NCHRP) report (Harwood, 2003). Speed-dependent maximum acceleration values for trucks with a 200 lb/hp weight-to-power ratio are shown in Table 3.1 (Pline, 1999; Ramezani et al., 2018; Yang et al., 2016). For maximum deceleration rate (also a part of truck vehicle-dynamics), the NHRCP report suggests values between 0.16g and 0.26g (where g = 9.8 m/sec^2) based on the worst and the best driver performance (Harwood, 2003). In this research, we consider 0.21g (2.06 m/sec^2) as the maximum deceleration, which is the average of the suggested values based on the best and the worst driver performance (Ramezani et al., 2018).

TABLE 3.1 Maximum Acceleration Rates for Heavy-Duty Trucks

Speed Range (mph)	**Speed Range (m/sec)**	**Maximum Acceleration (m/sec^2)**
0-10	0-4.4	0.55
10-20	4.4-8.9	0.49
20-30	8.9-13.3	0.40
30-40	13.3-17.8	0.24
40-50	17.8-22.2	0.15
>50	>22.2	0.12

CHAPTER FOUR

EVALUATION OF THE ASYMMETRIC LBCM

We evaluate the performance of the asymmetric LBCM in terms of platoon operational efficiency, i.e., how well the model can maintain a constant desired time headway, and stability by simulating a platoon of six fully automated trucks. In this study, a truck platoon represents a CACC platoon of fully automated trucks. To demonstrate the efficacy of this model, we compare the asymmetric LBCM with the symmetric LBCM.

4.1 Simulation Parameters and Evaluation Scenarios

In this study, we simulate a CACC platoon of six automated trucks (one leader and five follower trucks) in MATLAB for a total simulation time of 900 sec. The initial position of the leader truck is 300 m from the origin with the follower trucks positioned at 250 m, 200 m, 150 m, 100 m, and 50 m from the origin, respectively (as shown in Figure 4.1). The initial speed of all six trucks is 31.44 m/sec or 70.3 mph. In the simulation, the input parameters are the number of trucks in the platoon, the total simulation time, the initial position and speed of the follower trucks, the position and speed profile of the leader truck,

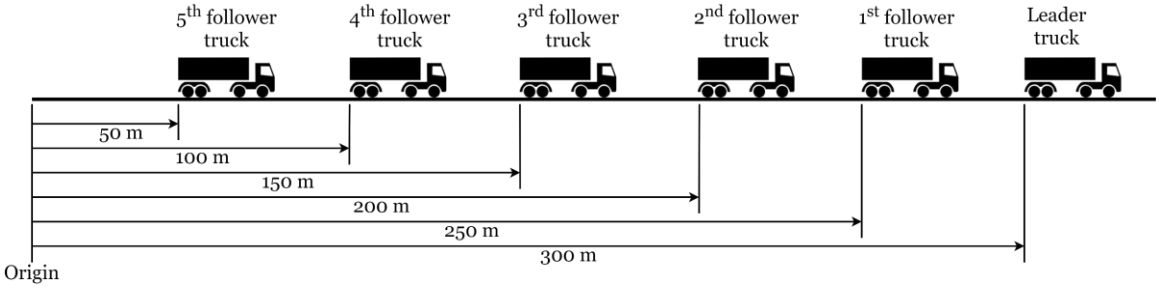

FIGURE 4.1 Initial position of the six automated trucks considered for evaluation of the asymmetric LBCM.

and the constant desired time headway. The simulation input parameters are summarized in Table 4.1.

TABLE 4.1 Summary of Simulation Scenario

Input Parameters	**Simulation Requirement**
Number of trucks in the platoon	One leader and five follower trucks
Initial position of the leader truck	300 m from the origin
Initial position of the follower trucks 1, 2, 3, 4, and 5	250 m, 200 m, 150 m, 100 m, and 50 m from the origin
Initial speed of the leader truck	31.44 m/sec (70.3 mph)
Initial speed of the follower trucks 1, 2, 3, 4, and 5	31.44 m/sec (70.3 mph)
Total simulation time	900 sec
Simulation step size	0.001 sec
Constant desired time headway	3 different settings: 0.6 sec, 0.8 sec, and 1.1 sec
Evaluation scenarios based on different traffic states defined by the leader truck	**Uniform speed or zero acceleration states** ▪ *State 1*: 31.44 m/sec (70.3mph) from 0 sec to 149 sec, 359 sec to 562 sec, and from 712 sec to 900 sec ▪ *State 2*: 19.69 m/sec (44.04 mph) from 158 sec to 240 sec ▪ *State 3*: 24.15 m/sec (54.02 mph) from 569 sec to 634 sec

Input Parameters	Simulation Requirement
	Non-linear acceleration states ▪ *State 1* (from 240 sec to 359 sec): Speed changes from 19.69 m/sec (44.04 mph) to 31.44 m/sec (70.3 mph) ▪ *State 2* (from 634 sec to 712 sec): Speed changes from 24.15 m/sec (54.02 mph) to 31.44 m/sec (70.3 mph) **Non-linear deceleration states** ▪ *State 1* (from 149 sec to 158 sec): Speed changes from 31.44 m/sec (54.02 mph) to 19.69 m/sec (44.04 mph) ▪ *State 2* (from 562 sec to 569 sec): Speed changes from 31.44 m/sec (74.3 mph) to 24.15 m/sec (54.02 mph)

The traffic states in the simulation are defined by the leader truck's speed profile, which is obtained from a calibrated traffic simulation network of the I-26 freeway in Berkeley, Orangeburg, and Dorchester County in South Carolina, developed by Rahman et al. (Rahman et al., 2015). The I-26 roadway network was created in PTV VISSIM traffic simulation software and calibrated based on collected field data to yield simulated volumes

and travel times within 10% of the actual volume and travel time data. The details of the network development and calibration can be found in (Rahman et al., 2015).

We use the truck vehicle dynamics described in section 3.3 as an input to the VISSIM I-26 network. We define two reduced speed areas (with speed limits of 55 mph and 45 mph) in the VISSIM I-26 network. Except for the two reduced speed areas, the other portions of the I-26 network have a speed limit of 75 mph. When the trucks enter one of the reduced speed areas, they must immediately reduce their speed and therefore undergo a sharp non-linear deceleration period. As the leader truck's speed profile is selected from one of the trucks of this network, the reduced speed areas define various traffic states based on the leader truck's speed profile. Table 4.1 summarizes different evaluation scenarios depending on the traffic states, which are defined by the selected truck's speed profile from VISSIM. The following assumptions are made for the evaluation scenarios,

- All the trucks in the platoon operate on a single lance,
- There is no cut-in traffic,
- The roads do not have any vertical or horizontal curvature,
- Once the platoon is formed, i.e., all the follower trucks achieve the desired time headway with their immediate leading trucks, no trucks attempt to merge with or diverge from the platoon, and
- The follower trucks receive the location and speed information of their immediate neighboring trucks in real-time without any noticeable delay.

4.2 Control Gain Estimation

To estimate the control gains of the symmetric and asymmetric LBCMs for an automated truck platoon, we focus on minimizing (i) the deviation of the follower trucks' speed from their immediate leading truck's speed, and (ii) the deviation of the follower trucks' time headway of from the desired time headway. For both LBCMs, there are three control gains to estimate: (i) relative distance gain, k_d (for the asymmetric LBCM, we consider $k_{d1} = k_{d2} = k_d$ for simplicity of design, and for the symmetric LBCM, $k_{d1} = k_d$ and k_{d2} is set to zero as the symmetric LBCM does not incorporate the constant desired time headway feature); (ii) relative speed gain, k_v, and (iii) feedback gain based on $(v_{des} - v_c)$, k_c.

We use the Genetic Algorithm (GA) for estimating the control gains of the symmetric and asymmetric LBCMs. The GA, developed by Holland, is a metaheuristic optimization method that mimics the process of natural selection and natural genetics (Goldberg and Holland, 1988; Holland, 1992). The GA can be used for both constrained (i.e., when the lower and upper bounds of the decision variables are specified) and unconstrained (i.e., when the lower and upper bounds of the decision variables are not specified) optimization problems. We apply GA in this study only to estimate the control gains as it is a global optimization algorithm that can globally optimize a multi-objective fitness function while satisfying non-linear inequality constraints, such as the constraint in (12). Besides, GA has been widely used in the literature to calibrate microscopic simulation models (Kim and Rilett, 2001; Ma and Abdulhai, 2002; Park and Qi, 2005; Schultz and Rilett, 2004).

To initialize the GA-based optimization for control gain estimation, we choose a population size of 50 candidate solutions, i.e., in each population, 50 candidate solutions are generated, which are evaluated based on the fitness function. As the number of decision variables is less than five for both LBCMs, a population size of 50 candidate solutions is sufficient. We define the two objectives of the multi-objective fitness function (y) as follows: (i) $y(1)$: the root mean squared errors (RMSE) of the follower trucks' speed with respect to their immediate leading trucks' speed, and (ii) $y(2)$: the RMSE of the follower trucks' time headways with respect to the constant desired time headway ($T_{h,des}$), which can be written as follows,

$$y(1) = \sqrt{\frac{(v_L - v_1)^2 + (v_1 - v_2)^2 + \cdots + (v_{i-1} - v_i)^2 + \cdots + (v_{N-1} - v_N)^2}{N}} \tag{13}$$

$$y(2) = \sum_{i=1}^{N} \sqrt{\frac{\left(T_{h,des} - T_{h,i}\right)^2}{N}} \tag{14}$$

where N is the total number of follower trucks; v_L and v_i, are the speeds of the leader truck of the platoon and the i-th follower truck, respectively; and $T_{h,i}$ is the actual time headway of the i-th follower truck with its immediate leading truck.

We use a separate simplified leader truck speed profile with linear accelerations and decelerations only for the control gain estimation purpose (as shown in Figure 4.2). As observed from Figure 3.4, the string stability region for $T_{h,des}$ = 0.6 sec is the most conservative among the three different time headway settings used for the evaluation section in this study, i.e., a set of control gains that satisfy the string stability condition for $T_{h,des}$ = 0.6 sec would also satisfy any other desired time headway setting for platooning

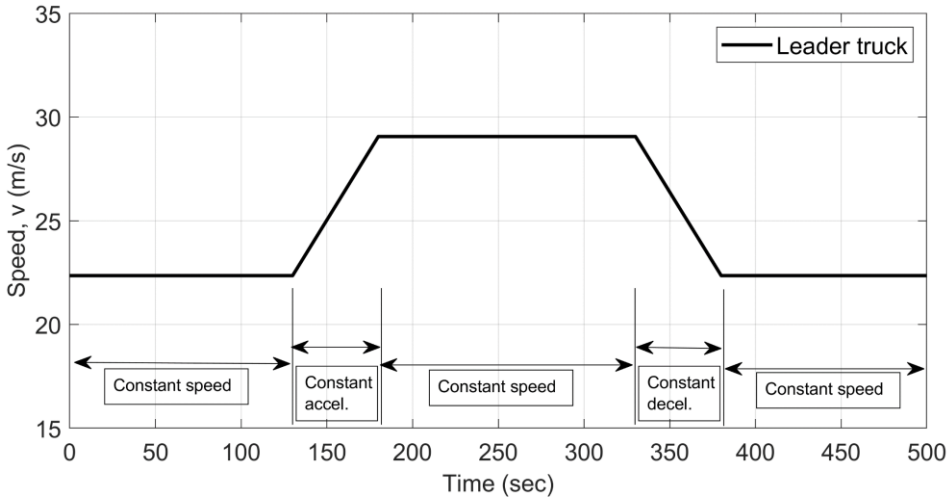

FIGURE 4.2 Speed profile of the leader truck for control gain estimation.

that is greater than 0.6 sec. Thus, we consider $T_{h,des}$ = 0.6 sec in (12) for estimating the control gains for both symmetric and asymmetric LBCMs through the GA optimization.

Table 4.2 presents a summary of the control gains obtained from the GA optimization that minimizes the fitness function defined in (13) and (14) for the leader truck's speed profile presented in Figure 4.2.

TABLE 4.2 Summary of Control Gains

Control Gains	**Values**
Symmetric LBCM	
Relative distance gain, k_d	0.8322 sec^{-2}
Relative speed gain, k_v	1.6170 sec^{-1}
Feedback gain based on $(v_c - v_{des})$, k_c	9.927e-4 sec^{-1}

Control Gains	Values
Asymmetric LBCM	
Relative distance gain, k_{d1}	1.9589 sec^{-2}
Relative headway gain, k_{d2}	1.9589 sec^{-2}
Relative speed gain, k_v	0.32 sec^{-1}
Feedback gain based on $(v_c - v_{des})$, k_c	0.04 sec^{-1}

4.3 Evaluation Metrics

To evaluate the fluctuation of time headway and speed for all the follower trucks, we introduce two evaluation metrics: (i) the sum of squared time headway error (SSTE), and (ii) the sum of squared speed error (SSSE). SSTE and SSSE at a given timestamp (t_i) are calculated as follows,

$$SSTE(t_i) = \sum_{j=1}^{N} \left(T_{h,j}(t_i) - T_{h,des}\right)^2 \tag{15}$$

$$SSSE(t_i) = \left(v_L(t_i) - v_1(t_i)\right)^2 + \sum_{j=2}^{N} \left(v_{j-1}(t_i) - v_j(t_i)\right)^2 \tag{16}$$

where, $T_{h,j}(t_i)$ is the actual time headway of the j^{th} follower truck at t_i with its immediate leading truck, $v_L(t_i)$ is the leader truck's speed at t_i, and $v_j(t_i)$ is the j^{th} follower truck's speed at t_i.

We choose to use the sum of the squared errors as it (i) magnifies the deviations of each follower truck from the desired behavior by squaring, and (ii) combines the errors or deviations of all the follower trucks by summing them up.

SSTE measures how well the follower trucks in the platoon can maintain a tightly coupled platoon formation compared to the constant desired time headway ($T_{h,des}$) when the speed of the leader truck changes. Thus, SSTE is also a representation of platoon operational efficiency here. SSTE = 0 at any timestamp, t_i indicates that all the follower trucks in the platoon maintain the desired time headway with their immediate leading trucks exactly without any deviation. A smaller inter-truck gap or time headway is essential to achieve higher platoon operational efficiency. Therefore, for a platoon of trucks, maintaining lower SSTE for a constant desired time headway allows the platoon to achieve higher platoon operational efficiency. A comparison of SSTE among the models can help to determine which model can provide higher platoon operational efficiency for a truck platooning application. For example, if model #1 yields an overall lower SSTE than model #2, then it can be concluded that model #1 provides higher platoon operational efficiency as compared to model #2.

SSSE measures the fluctuation of speed, i.e., SSSE = 0 indicates that all the follower trucks in the platoon follow their immediate leading truck's speed exactly without any error/deviation. The lower SSSE of a model compared to another can be an indicator of higher string stability. A platoon of trucks can be considered string stable when any non-zero speed error of any truck in the platoon does not get amplified in the upstream, i.e., in the follower trucks (Bose and Ioannou, 2001; Pueboobpaphan and Van Arem, 2010). Therefore, as SSSE is the sum of squared speed errors of all the follower trucks in the platoon with respect to their immediate leading truck at any given time, a comparison of SSSE profiles among the models can reveal the level of string stability rendered by one

model as compared to the other models. For example, if model #1 consistently yields lower SSSE than model #2, then it can be concluded that model #1 renders better string stability compared to model #2.

4.4 Evaluation Outcomes

In this subsection, we present the evaluation outcome of the asymmetric LBCM in terms of platoon operational efficiency, and local and string stability of an automated truck platoon. As explained previously, a CACC platoon of six automated trucks are simulated in a 900-sec simulation scenario with three different desired time headway settings, i.e., $T_{h,des}$ = 0.6 sec, 0.8 sec, and 1.1 sec, to investigate the efficacy of the asymmetric LBCM numerically. The platoon of six trucks (one leader truck and five follower trucks) are simulated in MATLAB by solving a system of first-order differential equations. We follow the same procedure as explained by Rahman et al. (Rahman et al., 2017) to form a system of first-order differential equations and use the "ode45" MATLAB solver. The simulation scenarios and the control gains used in the simulation experiment are presented in Tables 4.1 and 4.2, respectively.

4.4.1 Operational Efficiency of the Automated Truck Platoon

Figures 4.3 to 4.5 present the speed profiles of the trucks in an automated platoon for $T_{h,des}$ = 0.6 sec, 0.8 sec, and 1.1 sec, respectively, where the follower trucks in the platoon use the symmetric LBCM, and the asymmetric LBCM. We observe the performance of the asymmetric LBCM under non-linear acceleration and deceleration states to evaluate how well this linear model can handle non-linearity imposed by heavy-

duty trucks' vehicle dynamics. The times when the leader truck enters the reduced speed areas and brakes hard to keep its speed within the reduced speed requirement can be considered as critical evaluation scenarios. In the case of asymmetric LBCM, all the follower trucks are observed to be able to follow the leader truck's speed profile without any noticeable deviation throughout the entire simulation time for all three desired time headway settings (Figures 4.3 to 4.5).

However, in the case of the symmetric LBCM, the follower trucks require a short period of time following the end of the deceleration states to regain uniform speed for $T_{h,des}$ = 0.6 sec, and 0.8 sec (as denoted in Figures 4.3 and 4.4), whereas the follower trucks that use the asymmetric LBCM can almost immediately regain uniform speed following the deceleration states. Figures 4.3 to 4.5 illustrate that although the asymmetric LBCM is a linear control model, it can still capture the non-linear acceleration and deceleration states of a heavy-duty truck. In addition, the follower trucks that use the asymmetric LBCM experience significantly lower fluctuation in follower trucks' speed with respect to the leader truck's speed profile compared to the symmetric LBCM.

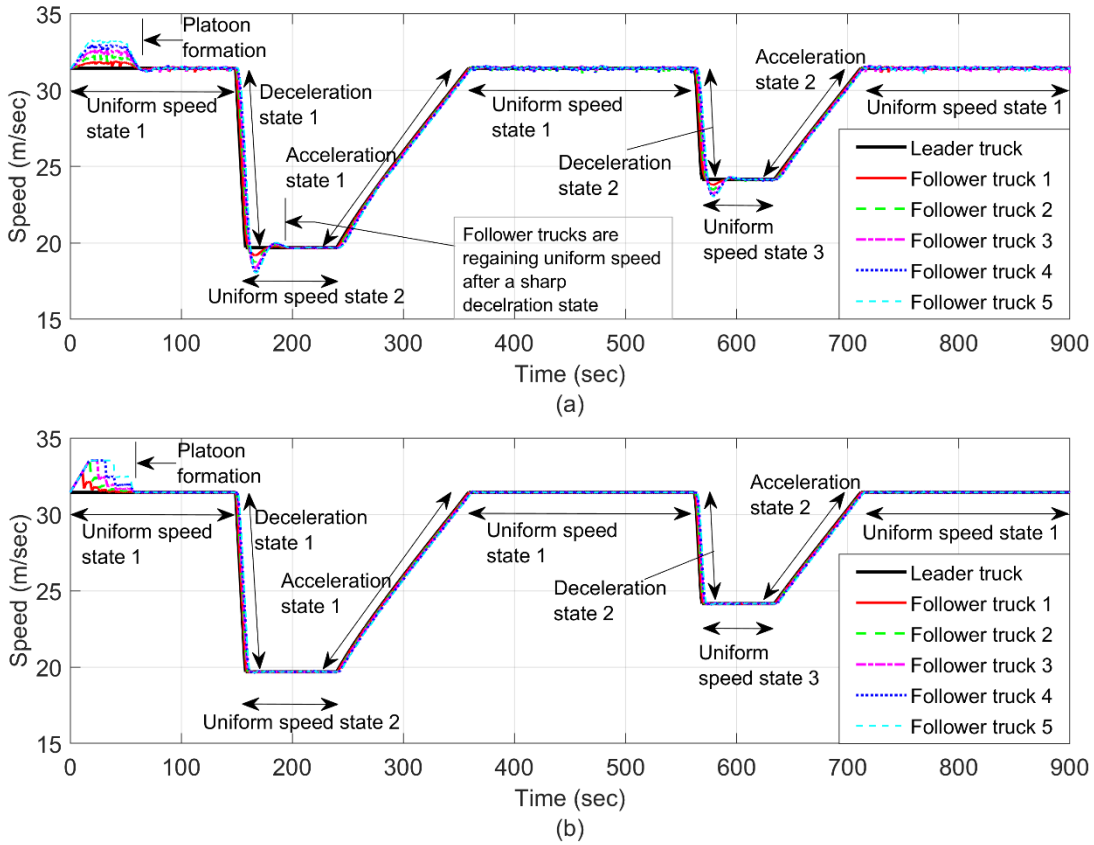

FIGURE 4.3 Speed profiles of the automated trucks using (a) the symmetric LBCM, and (b) the asymmetric LBCM for $T_{h,des} = 0.6$ sec.

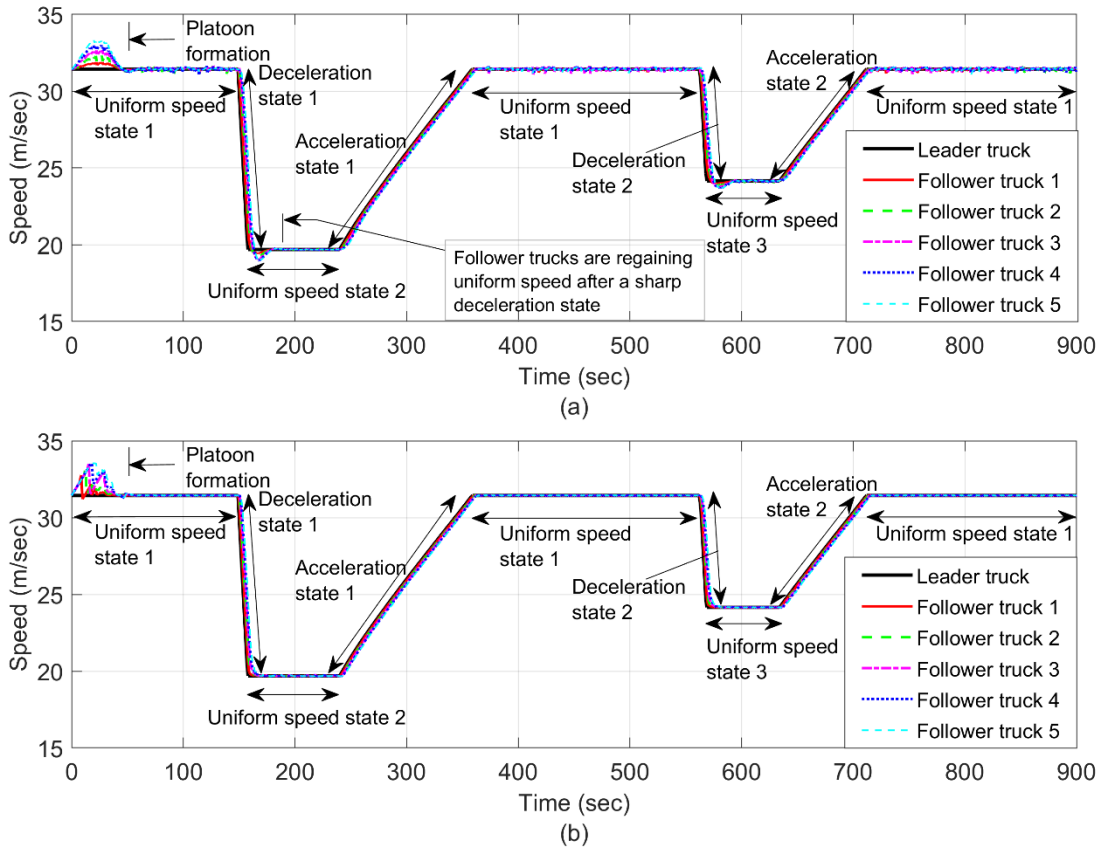

FIGURE 4.4 Speed profiles of the automated trucks using (a) the symmetric LBCM, and (b) the asymmetric LBCM for $T_{h,des} = 0.8$ sec.

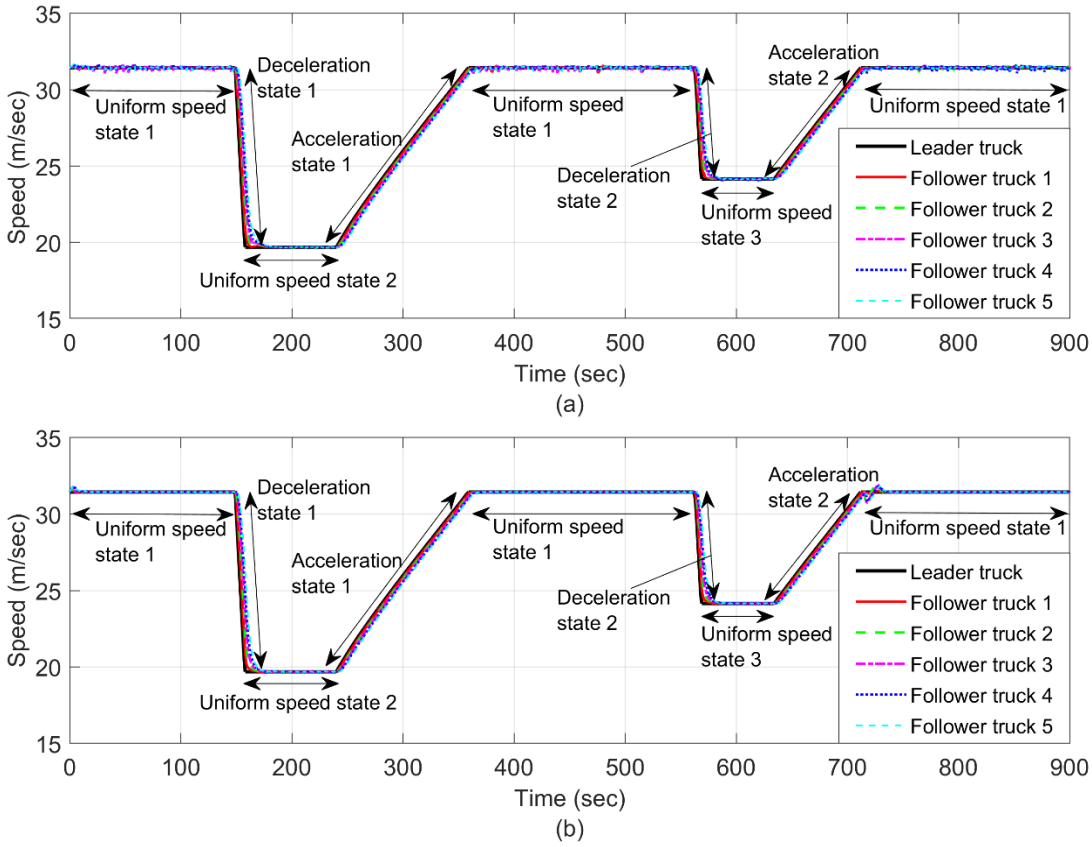

FIGURE 4.5 Speed profiles of the automated trucks using (a) the symmetric LBCM, and (b) the asymmetric LBCM for $T_{h,des} = 1.1$ sec.

Figures 4.6 to 4.8 present inter-truck gap profiles between every two trucks in the platoon that for $T_{h,des}$ = 0.6 sec, 0.8 sec, and 1.1 sec, respectively. First, as none of the inter-truck gaps shows zero or negative value, it can be concluded that there is no collision risk among the trucks in the platoon. Also, the inter-truck gap profiles show that all the follower trucks using the asymmetric LBCM can maintain the minimum safe gap of 10 m from their immediate leading truck at all times. Overall, all the follower trucks that use the asymmetric LBCM maintain uniform gaps across the platoon for all three desired time

headway settings. In the case of the symmetric LBCM, the follower trucks can maintain uniform gaps for $T_{h,des}$ = 1.1 sec, as observed from Figure 4.8. For $T_{h,des}$ = 0.8 sec, the symmetric LBCM cannot ensure uniform gaps at all times (see Figure 4.7), and for $T_{h,des}$ = 0.6 sec, some of the follower trucks fail to maintain the minimum safe gap of 10 m when the follower trucks try to regain uniform speed following a sharp deceleration state (denoted in Figure 4.6).

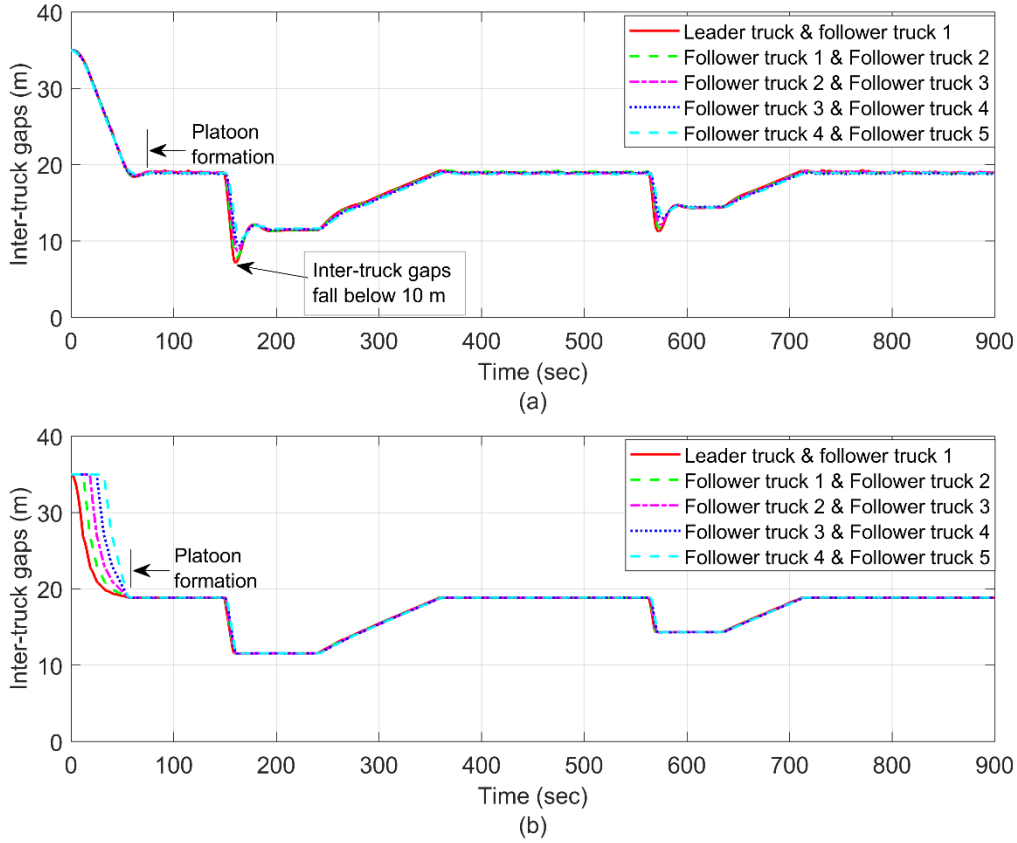

FIGURE 4.6 Inter-truck gap profiles using (a) the symmetric LBCM, and (b) the asymmetric LBCM for $T_{h,des}$ = 0.6 sec.

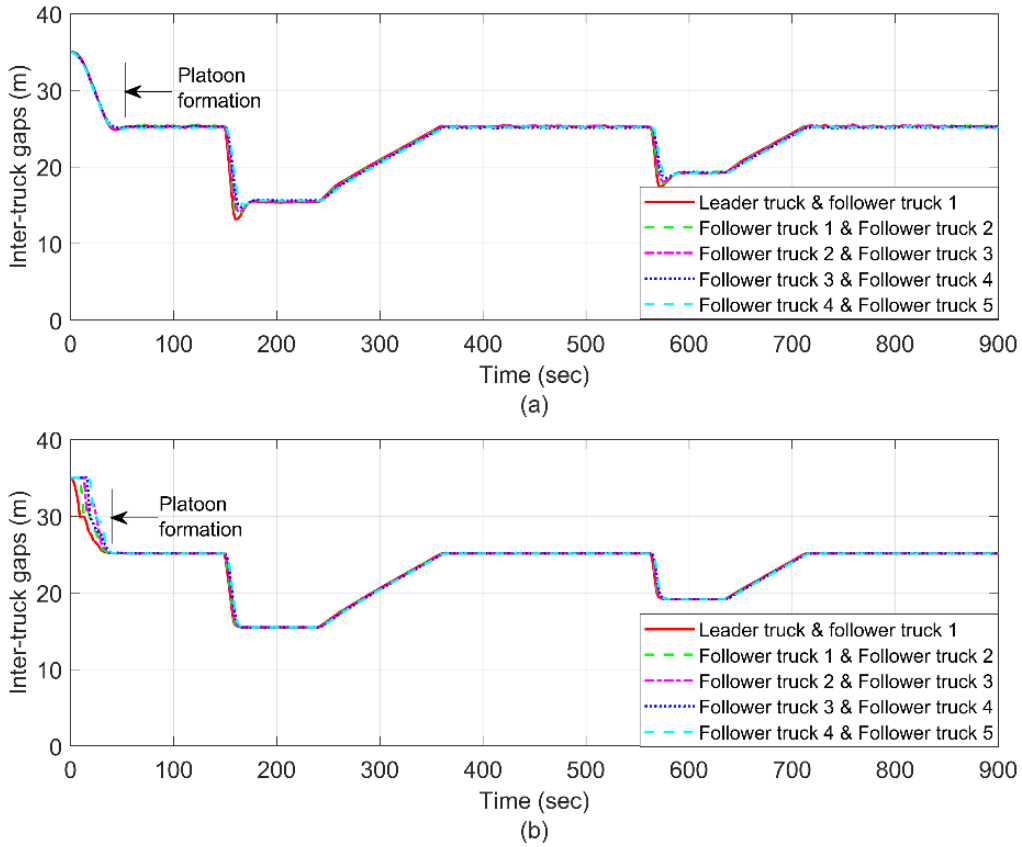

FIGURE 4.7 Inter-truck gap profiles using (a) the symmetric LBCM, and (b) the asymmetric LBCM for $T_{h,des} = 0.8$ sec.

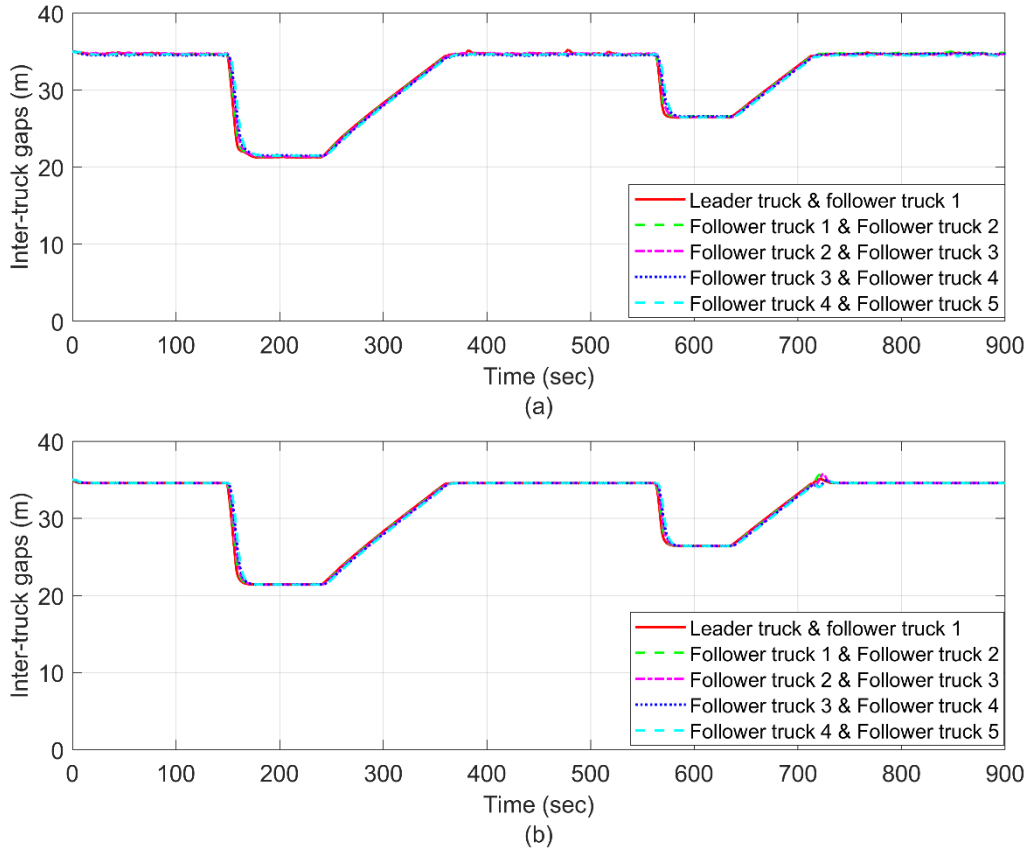

FIGURE 4.8 Inter-truck gap profiles using (a) the symmetric LBCM, and (b) the asymmetric LBCM for $T_{h,des} = 1.1$ sec.

Figures 4.9 to 4.11 present the time headway profile for each follower truck in the platoon. As seen from Figures 4.9 to 4.11, the asymmetric LBCM can consistently render the constant desired time headways without any significant deviation for all three desired time headway settings. In the case of the asymmetric LBCM, the desired time headway is maintained consistently only for $T_{h,des}$ = 1.1 sec (as observed in Figure 4.11). In Figure 4.9, the symmetric LBCM causes time headway to fall below the desired time headway, i.e., 0.8 sec, and the time headway between some trucks become critically low (below 0.5 sec) at times when the follower trucks try to regain uniform speed following the sharp

deceleration states. As the asymmetric LBCM can make the automated trucks in the platoon consistently follow a desired time headway without causing such safety issues, it will effectively provide higher throughput for the truck platoon. Thus, it indicates that the asymmetric LBCM is more operationally efficient for an automated truck platoon in terms of throughput without causing any safety issues compared to the symmetric LBCM.

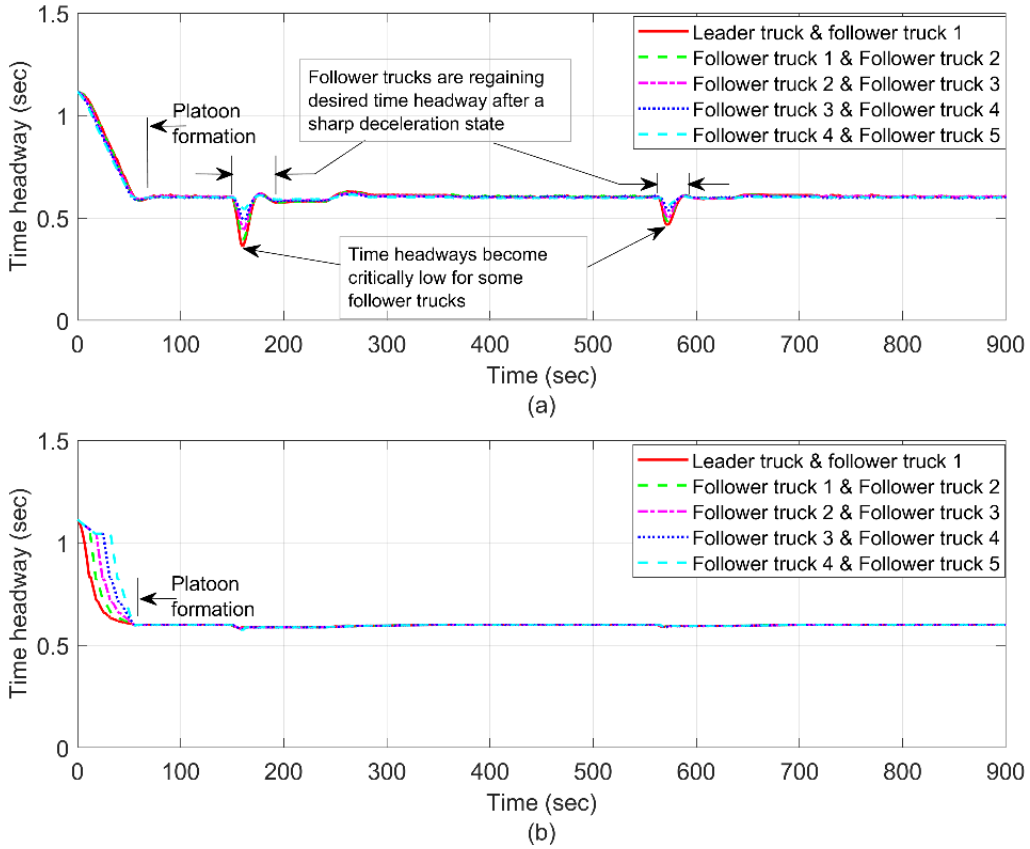

Figure 4.9 Time headway profiles for the follower trucks using (a) the symmetric LBCM, and (b) the asymmetric LBCM for $T_{h,des} = 0.6$ sec.

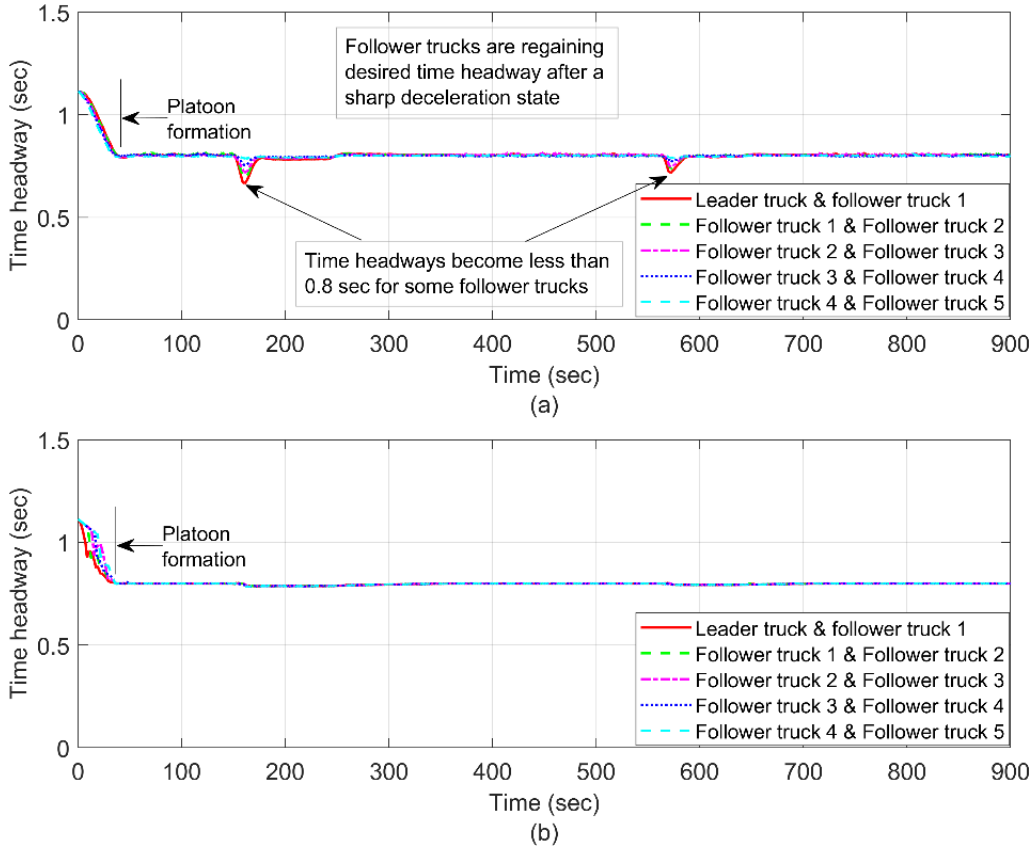

Figure 4.10 Time headway profiles for the follower trucks using (a) the symmetric LBCM, and (b) the asymmetric LBCM for $T_{h,des} = 0.8$ sec.

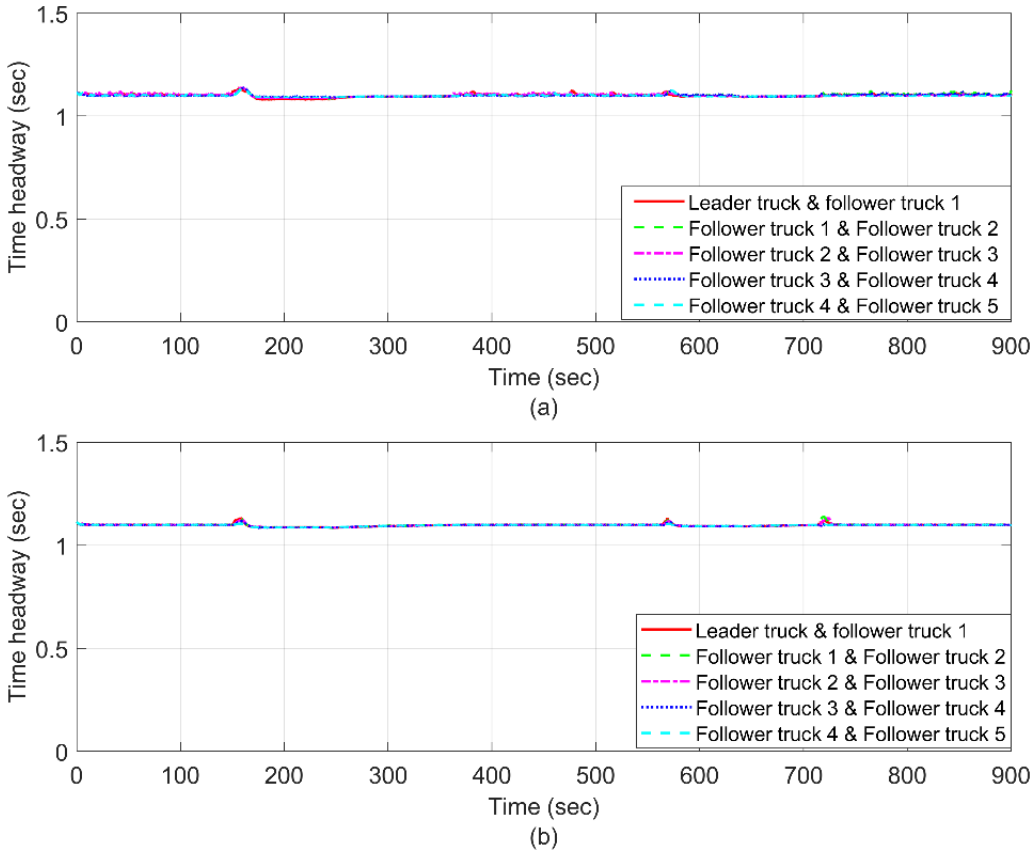

FIGURE 4.11 Time headway profiles for the follower trucks using (a) the symmetric LBCM, and (b) the asymmetric LBCM for $T_{h,des} = 1.1$ sec.

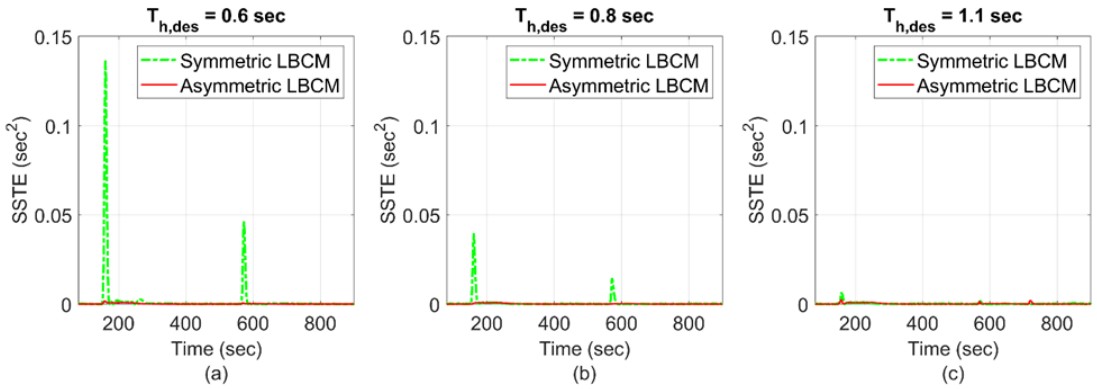

FIGURE 4.12 SSTE profiles of the automated trucks for (a) $T_{h,des} = 0.6$ sec, (b) $T_{h,des} = 0.8$ sec, and (c) $T_{h,des} = 1.1$ sec.

Figure 4.12 presents the sum of squared error profiles related to time headway (SSTE) for all three desired time headway settings. In calculating the sum of squared errors, we exclude the first 80 sec of the data, as it is considered as the stable platoon formation time window. As observed from Figure 4.12, SSTE ≈ 0 over the entire simulation period for the asymmetric LBCM, i.e., the SSTE profile indicates that all the follower trucks in the platoon that uses the asymmetric LBCM can maintain a constant desired time headway without any noticeable deviation unlike the symmetric LBCM in all traffic states. Therefore, the asymmetric LBCM can effectively provide higher operational efficiency for an automated truck platoon by keeping minimum time headway error.

4.4.2 Local Stability and String Stability of the Automated Truck Platoon

As explained in the Evaluation Metrics subsection, we utilize SSSE profiles to numerically validate the string stability of the automated truck platoon. Figure 4.13 compares the SSSE profiles between the symmetric and asymmetric LBCMs. For all three

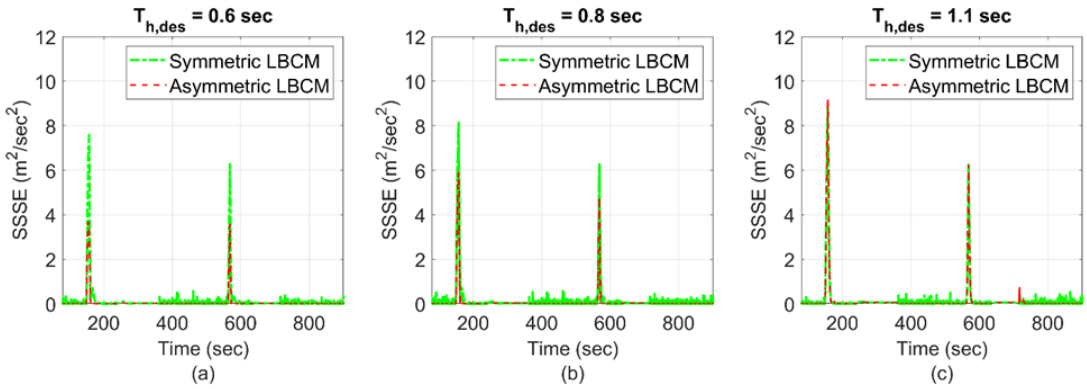

FIGURE 4.13 SSSE profiles of the automated trucks for (a) $T_{h,des} = 0.6$ sec, (b) $T_{h,des} = 0.8$ sec, and (c) $T_{h,des} = 1.1$ sec.

desired time headway settings, the asymmetric LBCM demonstrates lower SSSE. Note that, except for the two short periods of time following the two non-linear deceleration states (when the follower trucks try to regain uniform speed, as denoted in Figures 4.3 to 4.5), the asymmetric LBCM yields SSSE ≈0. Also, even in these two short periods of time, the SSSE for the asymmetric LBCM remains lower than the symmetric LBCM. Therefore, the asymmetric LBCM provides better string stability than the symmetric LBCM in all traffic states for all three desired time headway settings used in this study.

We further validate the local stability of the asymmetric LBCM by introducing perturbations in the leader truck's speed profile. We consider the smallest desired time headway among the three desired time headway settings used in this study, i.e., $T_{h,des}$ = 0.6 sec, for this local stability experiment. As mentioned before, a platoon of trucks using a BCM can be considered locally stable if any perturbation imposed by a truck in the platoon does not cause an increase in speed fluctuations over time for its upstream (i.e.,

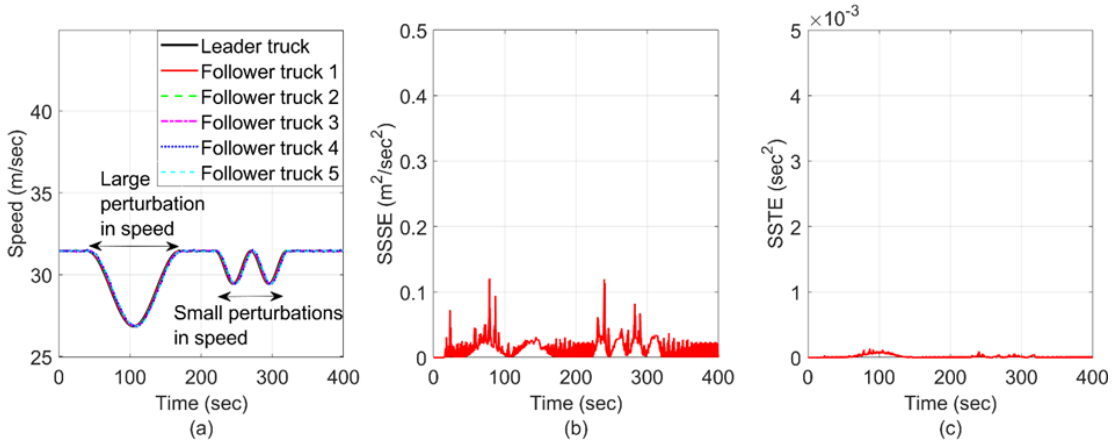

FIGURE 4.14 (a) Speed, (b) SSSE, and (c) SSTE profiles using the asymmetric LBCM while perturbations in speed are imposed by the leader truck.

follower) trucks and downstream (i.e., leading) trucks. As shown in Figure 4.14(a), the perturbations imposed by the leader truck's speed do not cause an increase in the speed fluctuations of the follower trucks, i.e., the perturbations do not make the platoon unstable. The follower trucks keep following the leader truck's speed profile without any noticeable deviation (as further demonstrated by the SSSE profile in Figure 4.14(b)). Figure 4.14(c) presents the SSTE profile, which demonstrates that even under a situation when the leader truck's speed changes abruptly, the follower trucks that use the asymmetric LBCM can maintain the desired time headway consistently, which implies that all trucks in the platoon remain locally stable.

CHAPTER FIVE

CONCLUSIONS

In this study, we develop an asymmetric LBCM that enables a platoon of fully automated trucks to tightly maintain a given constant time headway. First, we analyze the stability (local and string stability) of the asymmetric LBCM theoretically. The local stability of the model is proved theoretically using the condition for asymptotic stability of an LTI system. For analyzing the string stability of the model, we use the space headway error attenuation condition to determine the regions of $\mathcal{L}_\infty$ string stability under various desired time headway settings. Further, we numerically investigate the efficacy of the asymmetric LBCM compared to the symmetric LBCM in terms of platoon operational efficiency and stability by simulating a CACC platoon of six automated trucks. To mimic the real-world freeway operation of trucks, different acceleration and deceleration states, such as uniform speed states (i.e., zero acceleration states), and non-linear acceleration and deceleration states, are simulated to evaluate the operational performance of an automated truck platoon that uses the asymmetric LBCM.

5.1 Summary Findings

Analyses reveal that the asymmetric LBCM can capture the non-linear acceleration and deceleration states under various desired time headway settings without any noticeable deviation compared to the symmetric LBCM. Each truck in the platoon that uses the asymmetric LBCM can closely follow the speed of the leader truck under all simulated

scenarios. To demonstrate the platoon operational efficiency of the asymmetric LBCM for truck platooning application, we compare the time headways of the follower trucks in a platoon with their immediate leading trucks for symmetric and asymmetric LBCMs. Overall, the follower trucks that use the asymmetric LBCM can maintain a given desired time headway consistently without ever causing the trucks in the platoon to experience lower time headways than the desired time headway, which may cause safety issues, whereas the follower trucks that use the symmetric LBCM sometimes experience lower time headways than the desired time headways. This indicates that the asymmetric LBCM is more operationally efficient for an automated truck platoon compared to the symmetric LBCM. In addition, the sum of squared time headway error (SSTE) and the sum of squared speed error (SSSE) are estimated, for both models, to numerically compare them for the level of platoon operational efficiency and string stability, respectively. Analyses reveal that the asymmetric LBCM has the minimum SSTE and SSSE compared to the baseline model, i.e., the symmetric LBCM for all traffic states under all three desired time headway settings considered in this study, i.e., 0.6 sec, 0.8 sec, and 1.1 sec. Consequently, it can be concluded that an automated truck platoon that uses the asymmetric LBCM provides better string stability compared to the symmetric LBCM. Further investigation using perturbation imposed by the leader truck reveals that our asymmetric LBCM renders better local stability compared to the symmetric LBCM.

5.2 Recommendation and Feasibility of Implementation

In this study, we focused on developing an asymmetric LBCM as a longitudinal controller for an "automated truck platoon". However, the developed model can be used for platooning applications of other types of vehicles, such as passenger cars and buses. To utilize the asymmetric LBCM that we developed in this study for other types of vehicles' platooning applications, one would have to retune the control gains considering the constraints imposed by vehicle dynamics (as presented in Chapter 4.2 for heavy-duty trucks).

To implement the asymmetric LBCM developed in this study in the real world, each vehicle should receive location and speed information from its immediate leading and immediate following vehicles. Thus, the vehicles should be equipped with some forward- and rear-facing sensors, such as radio detection and ranging (RADAR) sensors, which can measure the distance and speed of the immediate neighboring vehicles. Alternatively, this information can be exchanged via communication devices, such as cellular vehicle-to-everything (CV2X) direct communication devices.

5.3 Limitation and Future Research Direction

A limitation of this study is that it focuses on an automated truck platoon formation on a lane without considering trucks moving in and out of the platoon. Our future study will focus on integrating the asymmetric LBCM with trucks moving in and out of the platoon. Also, the model does not account for uncertainties in the system, heterogeneity of vehicles, and delay in communication present in a real-world environment. Future studies

will also include an evaluation of the efficacy of the asymmetric LBCM in the real world and any further extension or modification that may be required for throughput improvement for a heterogeneous platoon of vehicles in a real-world environment.

APPENDICES

Appendix A

String Stability Analysis of the Symmetric LBCM

String stability of the symmetric LBCM can be analyzed using the same framework used here for the asymmetric LBCM. The linearized expression for the symmetric LBCM is as follows,

$$a_c = k_{d1}(d_l - d_f) + k_v\left[(v_l - v_c) - (v_c - v_f)\right] + k_c(v_{des} - v_c) \tag{17}$$

The expression in (17) can be rewritten in a state-space representation using the mass-spring-damper system showed in Figure A-1 as follows,

$$\dot{x}_{L,1} = x_{L,2}$$

$$\dot{x}_{L,2} = \frac{u}{m} - \frac{k}{m}(x_{L,1} - x_{1,1}) - \frac{c}{m}(x_{L,2} - x_{1,2})$$

$$\dot{x}_{1,1} = x_{1,2}$$

$$\dot{x}_{1,2} = \frac{k}{m}(x_{L,1} - 2x_{1,1} + x_{2,1}) + \frac{c}{m}(x_{L,2} - 2x_{1,2} + x_{2,2})$$

$$\dot{x}_{2,1} = x_{2,2}$$

$$\dot{x}_{2,2} = \frac{k}{m}(x_{1,1} - 2x_{2,1} + x_{3,1}) + \frac{c}{m}(x_{1,2} - 2x_{2,2} + x_{3,2})$$

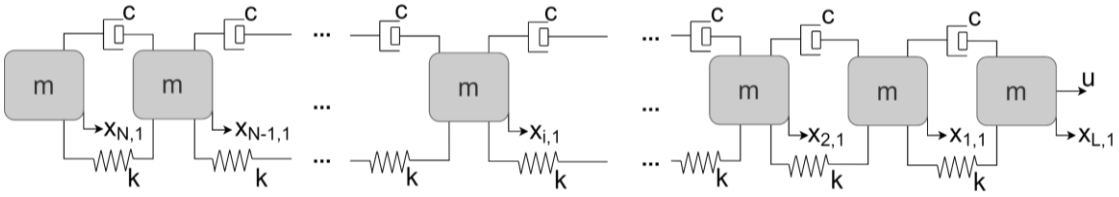

FIGURE A-1 Mass-spring-damper system representing a platoon of (N+1) automated trucks under symmetric LBCM.

$$\vdots$$

$$\dot{x}_{i,1} = x_{i,2}$$

$$\dot{x}_{i,2} = \frac{k}{m}\left(x_{i-1,1} - 2x_{i,1} + x_{i+1,1}\right) + \frac{c}{m}\left(x_{i-1,2} - 2x_{i,2} + x_{i+1,2}\right)$$

$$\vdots$$

$$\dot{x}_{N-1,1} = x_{N-1,2}$$

$$\dot{x}_{N-1,2} = \frac{k}{m}\left(x_{N-2,1} - 2x_{N-1,1} + x_{N,1}\right) + \frac{c}{m}\left(x_{N-2,2} - 2x_{N-1,2} + x_{N,2}\right)$$

$$\dot{x}_{N,1} = x_{N,2}$$

$$\dot{x}_{N,2} = \frac{k}{m}\left(x_{N-1,1} - x_{N,1}\right) + \frac{c}{m}\left(x_{N-1,2} - x_{N,2}\right) \tag{18}$$

where, $k_{d1} \triangleq \frac{k}{m}$, and $k_v = \frac{c}{m}$

The above state-space representation can be transformed into space headway error coordinates using the following transformations,

$$z_{1,1} = x_{L,1} - x_{1,1} - T_{h,des}x_{1,2}$$

$$z_{1,2} = \dot{z}_{1,1} = x_{L,2} - x_{1,2} - T_{h,des}\dot{x}_{1,2}$$

$$z_{2,1} = x_{1,1} - x_{2,1} - T_{h,des}x_{2,2}$$

$$z_{2,2} = \dot{z}_{2,1} = x_{1,2} - x_{2,2} - T_{h,des}\dot{x}_{2,2}$$

$$\vdots$$

$$z_{i,1} = x_{i,1} - x_{i+1,1} - T_{h,des}x_{i+1,2}$$

$$z_{i,2} = \dot{z}_{i,1} = x_{i,2} - x_{i+1,2} - T_{h,des}\dot{x}_{i+1,2}$$

$$\vdots$$

$$z_{N-2,1} = x_{N-2,1} - x_{N-1,1} - T_{h,des}x_{N-1,2}$$

$$z_{N-2,2} = \dot{z}_{N-2,1} = x_{N-2,2} - x_{N-1,2} - T_{h,des}\dot{x}_{N-1,2}$$

$$z_{N-1,1} = x_{N-1,1} - x_{N,1} - T_{h,des}x_{N,2}$$

$$z_{N-1,2} = \dot{z}_{N-1,1} = x_{N-1,2} - x_{N,2} - T_{h,des}\dot{x}_{N,2} \quad (19)$$

Then, the state-space representation of the space headway errors can be written as,

$$\dot{z}_{1,1} = z_{1,2}$$

$$\dot{z}_{1,2} = -\frac{2k}{m}z_{1,1} + \frac{k}{m}z_{2,1} - \frac{2c}{m}z_{1,2} + \frac{c}{m}z_{2,2}$$

$$\dot{z}_{2,1} = z_{2,2}$$

$$\dot{z}_{2,2} = \frac{k}{m}z_{1,1} - \frac{2k}{m}z_{2,1} + \frac{k}{m}z_{3,1} + \frac{c}{m}z_{1,2} - \frac{2c}{m}z_{2,2} + \frac{c}{m}z_{3,2}$$

$$\vdots$$

$$\dot{z}_{i,1} = z_{i,2}$$

$$\dot{z}_{i,2} = \frac{k}{m}z_{i-1,1} - \frac{2k}{m}z_{i,1} + \frac{k}{m}z_{i+1,1} + \frac{c}{m}z_{i-1,2} - \frac{2c}{m}z_{i,2} + \frac{c}{m}z_{i+1,2}$$

$$\vdots$$

$$\dot{z}_{N-2,1} = z_{N-2,2}$$

$$\dot{z}_{N-2,2} = \frac{k}{m}z_{N-3,1} - \frac{2k}{m}z_{N-2,1} + \frac{k}{m}z_{N-1,1} + \frac{c}{m}z_{N-3,2} - \frac{2c}{m}z_{N-2,2} + \frac{c}{m}z_{N-1,2}$$

$$\dot{z}_{N-1,1} = z_{N-1,2}$$

$$\dot{z}_{N-1,2} = \frac{k}{m}z_{N-2,1} - \frac{2k}{m}z_{N-1,1} + \frac{c}{m}z_{N-2,2} - \frac{2c}{m}z_{N-1,2} \quad (20)$$

As mentioned before, the conditions for string stability of a BCM can be derived by considering the last two masses in the mass-spring-damper system. The space headway error transfer function for the last two masses can be written from (20) as,

$$G(s) = \frac{z_{N-1,1}(s)}{z_{N-2,1}(s)} = \frac{\frac{c}{m}s + \frac{k}{m}}{s^2 + \left(\frac{2c}{m}\right)s + \frac{2k}{m}} \tag{21}$$

To ensure string stability of the symmetric LBCM, $|G(j\omega)| < 1, \forall\omega > 0$. From (21), it can be showed that $|G(j\omega)| < 1, \forall\omega > 0$, when,

$$\frac{c}{m} > \sqrt{\frac{(4+2\sqrt{3})k}{3m}} \tag{22}$$

which can be rewritten in terms of k_d and k_v (here, $k_{d1} \triangleq k_d$) as follows,

$$k_v > \sqrt{\frac{(4+2\sqrt{3})k_d}{3}} \tag{23}$$

The above inequality expression provides the condition for string stability of the symmetric LBCM. However, unlike the string stability condition for the asymmetric LBCM, (23) does not include $T_{h,des}$ as the symmetric LBCM does not include the desired time headway feature directly into the control model. Figure A-2 shows the regions of string stability (indicated with upward arrow) that corresponds to (23).

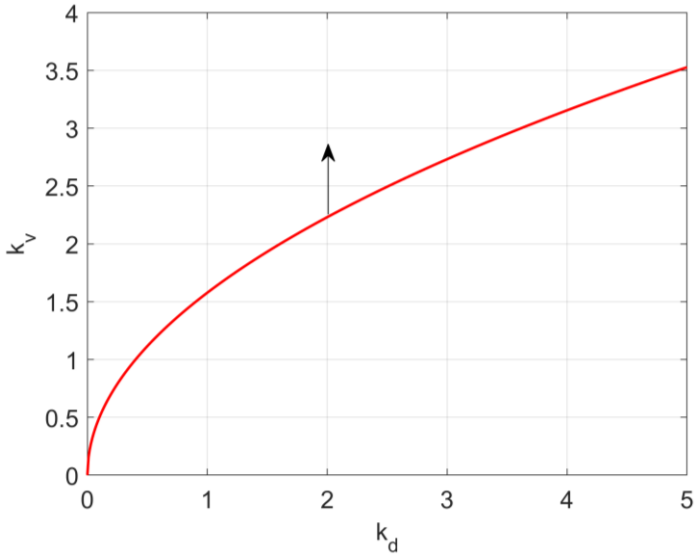

FIGURE A-2 Region of string stability for the symmetric LBCM in relative speed gain (k_v) vs. relative distance gain (k_d) plane.

Appendix B

MATLAB Code for Numerical Validation

```
%%%%%%%%%%%%%%%%%%%%%%%%%%%%%%%%%%%%%%%%%%%%%%%%%%%%%%%%%%%%%%%%%%%%%%%%%%%%
%%%%%%%%%%%%%%%%%%%%%%%%NUMERICAL VALIDATION%%%%%%%%%%%%%%%%%%%%%%%%%%%%%%%%
%%%%%%%%%%%%%%%%%%%%%%%%OF ASYMMETRIC LBCM%%%%%%%%%%%%%%%%%%%%%%%%%%%%%%%%%%
% % Written by M Sabbir Salek, msalek@clemson.edu


close all;
clear all; clc;
%%%%%%%%%% INPUT PARAMETERS
%%%%%%%%%% %%%%%%%%%%%%%%%%%%%%%%%%%%%%%%%%%%%%%%%%%%%%%%%%%%%%%%%%%%%%%%%%%%
N_truck = 5; %Number of Cars
l = 15; %Length of trucks
Th_const = 0.6;
%%%%%%%%%%%%%%%%%%%%%%%%%%%%%%%%%%%%%%%%%%%%%%%%%%%%%%%%%%%%%%%%%%%%%%%%%%%%


N = N_truck + 1


%%%%%%%%%% Position of car 0 with respect to time %%
Xfinal = zeros(0,0); %% Position of vehicle
Tfinal = zeros(0,0);
Vfinal = zeros(0,0);


%%%%%%%%%%%%%%%%%%%%%%%%%%%%%%%%%%%%%%%%%%%%%%%%%%%%%%%%%%%%%%%%%%%%%%%%%%%%


Vfinal = load('vissim_data_2_mod.txt');
```

```
Xprevious = 0;

F_time = size(Vfinal,1)-1;    % final time

xb = [0:1:F_time]';
xa = [0:0.1:F_time]';
Vfinal = interp1(xb, Vfinal, xa);

k = 0 ;
init_gap = 50;

    for i=0:0.1:F_time

        if i == 0
            s1 = init_gap*N;
            X = s1;
            Xprevious = s1;
        else
            s2 = ((Vfinal(k+1,1) + Vfinal(k,1))/2)*0.1;
            X = Xprevious + s2;
            Xprevious = X;
        end

        Xfinal=[Xfinal;X];
        Tfinal=[Tfinal;i];
```

```
        k = k +1;
    end

%%%%%%%%%%%%Initial Position and Velocity of Car 0 %%%%%%%%
    initial_values=zeros(2*N,1);

    for i=1:N
        initial_values(i)=(N-i)*init_gap;
        initial_values(i+N)=Vfinal(1,1);
    end

%%%%%%%%%%%%%%%%%%% SOLUTION OF SYSTEM OF EQUATIONS  %%%%%

tspan = 0:0.001:F_time;
kd_2 = 1.9589;
[Tbm,Ybm] = ode45( @(t,y) ...
    bmcarflw(t, y, N, Tfinal, Xfinal, Vfinal,kd_2, Th_const), tspan,
initial_values);

kd_2 = 0;
[Tbl,Ybl] = ode45( @(t,y) ...
    HornWang(t, y, N, Tfinal, Xfinal, Vfinal,kd_2, Th_const), tspan,
initial_values);

% ------------------------------------------------------------------
---------------------------
```

```
%%%%%%%%%%%%Plot HornWang ---Velocity%%%%%%%%%%%%%%%%
figure(1);
h(1) = subplot(2,3,1:3);
hold on;
builtin('plot',Tfinal,Vfinal,'k-','LineWidth', 2)
plot(Tbl,Ybl(:,N+1),'r-','Linewidth',1.5)
plot(Tbl,Ybl(:,N+2),'g--','Linewidth',1.5)
plot(Tbl,Ybl(:,N+3),'m-.','Linewidth',1.5)
plot(Tbl,Ybl(:,N+4),'b:','Linewidth',1.5)
plot(Tbl,Ybl(:,N+5),'c--','Linewidth',1,'MarkerSize',1.5)

xlabel(['Time (sec)',newline,'(a)'])
ylabel('Speed (m/sec)')
xlim([0 900])
ylim([15 35])
legend([builtin('plot',Tfinal,Vfinal,'k-','LineWidth', 2) ...
    plot(Tbl,Ybl(:,N+1),'r-','Linewidth',1.5) ...
    plot(Tbl,Ybl(:,N+2),'g--','Linewidth',1.5) ...
    plot(Tbl,Ybl(:,N+3),'m-.','Linewidth',1.5) ...
    plot(Tbl,Ybl(:,N+4),'b:','Linewidth',1.5) ...
    plot(Tbl,Ybl(:,N+5),'c--','Linewidth',1,'MarkerSize',1.5)], ...
    'Leader truck','Follower truck 1','Follower truck 2',...
    'Follower truck 3','Follower truck 4', 'Follower truck 5');
grid on
box on
% %%%%%%%%%%%%%%%%%%%%%%%%%%%%%%%%%%%%%%%%%%%%%%%%%%%%%%%%%%%%
%
```

```
% %%%%%%%%%%%%%%Plot ALBCM ---Velocity%%%%%%%%%%%%%%%%
figure(1);
h(2) = subplot(2,3,4:6);
hold on;
builtin('plot',Tfinal,Vfinal,'k-','LineWidth', 2)
plot(Tbm,Ybm(:,N+1),'r-','Linewidth',1.5)
plot(Tbm,Ybm(:,N+2),'g--','Linewidth',1.5)
plot(Tbm,Ybm(:,N+3),'m-.','Linewidth',1.5)
plot(Tbm,Ybm(:,N+4),'b:','Linewidth',1.5)
plot(Tbm,Ybm(:,N+5),'c--','Linewidth',1,'MarkerSize',1.5)

xlabel(['Time (sec)',newline,'(b)'])
ylabel('Speed (m/s)')
xlim([0 900])
ylim([15 35])
legend([builtin('plot',Tfinal,Vfinal,'k-','LineWidth', 2) ...
    plot(Tbm,Ybm(:,N+1),'r-','Linewidth',1.5) ...
    plot(Tbm,Ybm(:,N+2),'g--','Linewidth',1.5) ...
    plot(Tbm,Ybm(:,N+3),'m-.','Linewidth',1.5) ...
    plot(Tbm,Ybm(:,N+4),'b:','Linewidth',1.5) ...
    plot(Tbm,Ybm(:,N+5),'c--','Linewidth',1,'MarkerSize',1.5)], ...
    'Leader truck','Follower truck 1','Follower truck 2',...
    'Follower truck 3','Follower truck 4', 'Follower truck 5');
grid on
box on
% %%%%%%%%%%%%%%%%%%%%%%%%%%%%%%%%%%%%%%%%%%%%%%%%%%%%%%%%
%
```

```
set(findall(gcf,'-property','FontSize'),'FontSize',18)
%
%%%%%%%%%%%%%%%%%%%%%%%%%%%%%%%%%%%%%%%%%%%%%%%%%%%%%%%%%

[r,c] = size(Ybm);
gap_bl = zeros(r, N-1);
gap_bm = zeros(r, N-1);

tb = 0:0.1:F_time;
ta = 0:0.001:F_time;
Yleader = interp1(tb, Xfinal, ta);
Yleader = Yleader';
Vleader = interp1(tb, Vfinal, ta);
Vleader = Vleader';

for i = 1:N-1
    if i == 1
        gap_bl(:,i) = Yleader(:,1) - Ybl(:,i) - l;
        gap_bm(:,i) = Yleader(:,1) - Ybm(:,i) - l;
    else
        gap_bl(:,i) = Ybl(:,i-1) - Ybl(:,i) - l;
        gap_bm(:,i) = Ybm(:,i-1) - Ybm(:,i) - l;
    end
end

Th_bl = zeros(r, N-1);
Th_bm = zeros(r, N-1);
```

```
for i = 1:N-1      % from 1 to 4 for N=6
    Th_bl(:,i) = gap_bl(:,i)./Ybl(:,i+N);
    Th_bm(:,i) = gap_bm(:,i)./Ybm(:,i+N);
end

% %%%%%%%%%%%%%%%%%%%%%%%%%%%%%%%%%%%%%%%%%%%%%%%%%%%%%%%%%%%%%%%%%%%
%
%%%%%%%%%%%%%Plot HornWang ---Gap %%%%%%%%%%%%%%%
figure(2);
subplot(2,3,1:3);
hold on;
plot(Tbl,gap_bl(:,1),'r-','Linewidth',1.5)
plot(Tbl,gap_bl(:,2),'g--','Linewidth',1.5)
plot(Tbl,gap_bl(:,3),'m-.','Linewidth',1.5)
plot(Tbl,gap_bl(:,4),'b:','Linewidth',1.5)
plot(Tbl,gap_bl(:,5),'c--','Linewidth',1.5)

xlabel(['Time (sec)',newline,'(a)'])
ylabel('Inter-truck gaps (m)')
ylim([0 40])
xlim([0 F_time])
legend([plot(Tbl,gap_bl(:,1),'r-','Linewidth',1.5) ...
    plot(Tbl,gap_bl(:,2),'g--','Linewidth',1.5) ...
    plot(Tbl,gap_bl(:,3),'m-.','Linewidth',1.5) ...
    plot(Tbl,gap_bl(:,4),'b:','Linewidth',1.5) ...
    plot(Tbl,gap_bl(:,5),'c--','Linewidth',1.5)], ...
```

```
    'Leader truck & follower truck 1','Follower truck 1 & Follower
truck 2', ...
    'Follower truck 2 & Follower truck 3','Follower truck 3 & Follower
truck 4', ...
    'Follower truck 4 & Follower truck 5');
grid on;
box on;
% %%%%%%%%%%%%%%%%%%%%%%%%%%%%%%%%%%%%%%%%%%%%%%%%%%%%%%%%%%%%%%%%%%%

% %%%%%%%%%%%%%%Plot ALBCM ---Gap %%%%%%%%%%%%%%%
figure(2);
subplot(2,3,4:6);
hold on;
plot(Tbm,gap_bm(:,1),'r-','Linewidth',1.5)
plot(Tbm,gap_bm(:,2),'g--','Linewidth',1.5)
plot(Tbm,gap_bm(:,3),'m-.','Linewidth',1.5)
plot(Tbm,gap_bm(:,4),'b:','Linewidth',1.5)
plot(Tbm,gap_bm(:,5),'k--','Linewidth',1.5)

xlabel(['Time (sec)',newline,'(b)'])
ylabel('Inter-truck gaps (m)')
ylim([0 40])
xlim([0 F_time])
legend([plot(Tbm,gap_bm(:,1),'r-','Linewidth',1.5) ...
    plot(Tbm,gap_bm(:,2),'g--','Linewidth',1.5) ...
    plot(Tbm,gap_bm(:,3),'m-.','Linewidth',1.5) ...
    plot(Tbm,gap_bm(:,4),'b:','Linewidth',1.5) ...
```

```
    plot(Tbm,gap_bm(:,5),'c--','Linewidth',1.5)], ...
    'Leader truck & follower truck 1','Follower truck 1 & Follower
truck 2', ...
    'Follower truck 2 & Follower truck 3','Follower truck 3 & Follower
truck 4', ...
    'Follower truck 4 & Follower truck 5');
grid on;
box on;

set(findall(gcf,'-property','FontSize'),'FontSize',14)

%%%%%%%%%%%%%%%%%%%%%%%%%%%%%%%%%%%%%%%%%%%%%%%%%%%%%%%%%%%%%%%%%%%%

%%%%%%%%%%%%Plot BL ---Time headway %%%%%%%%%%%%%%%

figure(3);
subplot(2,3,1:3);
hold on;
plot(Tbl,Th_bl(:,1),'r-','Linewidth',1.5)
plot(Tbl,Th_bl(:,2),'g--','Linewidth',1.5)
plot(Tbl,Th_bl(:,3),'m-.','Linewidth',1.5)
plot(Tbl,Th_bl(:,4),'b:','Linewidth',1.5)
plot(Tbl,Th_bl(:,5),'c--','Linewidth',1.5)

xlabel(['Time (sec)',newline,'(a)'])
ylabel('Time headway (sec)')
ylim([0 1.5])
yticks([0 0.5 1 1.5 2])
```

```
xlim([0 F_time])
legend([plot(Tbl,Th_bl(:,1),'r-','Linewidth',1.5)...
        plot(Tbl,Th_bl(:,2),'g--','Linewidth',1.5)...
        plot(Tbl,Th_bl(:,3),'m-.','Linewidth',1.5)...
        plot(Tbl,Th_bl(:,4),'b:','Linewidth',1.5)...
        plot(Tbl,Th_bl(:,5),'c--','Linewidth',1.5)], ...
    'Leader truck & follower truck 1','Follower truck 1 & Follower
truck 2', ...
    'Follower truck 2 & Follower truck 3','Follower truck 3 & Follower
truck 4', ...
    'Follower truck 4 & Follower truck 5');
grid on;
box on;
%%%%%%%%%%%%%%%%%%%%%%%%%%%%%%%%%%%%%%%%%%%%%%%%%%%%%%%%%%%%%%%%%%%%%%%

%%%%%%%%%%%%%%Plot ALBCM ---Time headway %%%%%%%%%%%%%%%%
figure(3);
subplot(2,3,4:6);
hold on;
plot(Tbm,Th_bm(:,1),'r-','Linewidth',1.5)
plot(Tbm,Th_bm(:,2),'g--','Linewidth',1.5)
plot(Tbm,Th_bm(:,3),'m-.','Linewidth',1.5)
plot(Tbm,Th_bm(:,4),'b:','Linewidth',1.5)
plot(Tbm,Th_bm(:,5),'c--','Linewidth',1.5)

xlabel(['Time (sec)',newline,'(b)'])
ylabel('Time headway (sec)')
```

```
ylim([0 1.5])
yticks([0 0.5 1 1.5 2])
xlim([0 F_time])
legend([plot(Tbm,Th_bm(:,1),'r-','Linewidth',1.5)...
        plot(Tbm,Th_bm(:,2),'g--','Linewidth',1.5)...
        plot(Tbm,Th_bm(:,3),'m-.','Linewidth',1.5)...
        plot(Tbm,Th_bm(:,4),'b:','Linewidth',1.5)...
        plot(Tbm,Th_bm(:,5),'c--','Linewidth',1.5)], ...
    'Leader truck & follower truck 1','Follower truck 1 & Follower
truck 2', ...
    'Follower truck 2 & Follower truck 3','Follower truck 3 & Follower
truck 4', ...
    'Follower truck 4 & Follower truck 5');
grid on;
box on;

set(findall(gcf,'-property','FontSize'),'FontSize',14)



%%%%%%%%%%%%%%%%%%%%%%%%%%%%%%%%%%%%%%%%%%%%%%%%%%%%%%%%%%%%%%%%%%%%%%%
% %%%%%%%%%%%%%%%%%%%%%%%% Plot SSSE %%%%%%%%%%%%%%%%%%%%%%%%%%%%%%%%%%

E_vel_bl = [Vleader, Ybl(:,N+1:N+N_truck-1)] - Ybl(:,N+1:N+N_truck);
E_vel_bm = [Vleader, Ybm(:,N+1:N+N_truck-1)] - Ybm(:,N+1:N+N_truck);

SSE_vel_bl = sum(E_vel_bl.^2, 2);
SSE_vel_bm = sum(E_vel_bm.^2, 2);
```

```
figure(4);
% subplot(1,3,1);
hold on
plot(Tbl(80001:end),SSE_vel_bl(80001:end),'g-.','LineWidth',2)
plot(Tbm(80001:end),SSE_vel_bm(80001:end),'r--','LineWidth',1.5)

xlabel(['Time (sec)',newline,'(a)'])
xlim([80 900])
ylim([0 12])
ylabel('SSSE (m^2/sec^2)')
legend([plot(Tbl(80001:end),SSE_vel_bl(80001:end),'g-.','LineWidth',2)
...
    plot(Tbl(80001:end),SSE_vel_bm(80001:end),'r--','LineWidth',1.35)],
...
    'Symmetric LBCM', 'Asymmetric LBCM');
title('T_{h,des} = 0.6 sec');
grid on
box on

set(findall(gcf,'-property','FontSize'),'FontSize',16);



%%%%%%%%%%%%%%%%%%%%%%%%%%%%%%%%%%%%%%%%%%%%%%%%%%%%%%%%%%%%%%%%%%%%%%%%%%%%%%%

SSE_Th_bl = sum((Th_bl-Th_const).^2, 2);
SSE_Th_bm = sum((Th_bm-Th_const).^2, 2);
```

```
%%%%%%%%%%%%%%%%%%%%%%%%%%%%%%%%%%%%%%%%%%%%%%%%%%%%%%%%%%%%%%%%%%%%%%%
%%%%%%%%%%%%%%%%%%%%%%%%    SSTE    %%%%%%%%%%%%%%%%%%%%%%%%%%%%%%%%%%
figure(5);
% subplot(1,3,3);
hold on
plot(Tbl(80001:end),SSE_Th_bl(80001:end),'g-.','LineWidth',2)
plot(Tbm(80001:end),SSE_Th_bm(80001:end),'r-','LineWidth',1.5)

xlabel(['Time (sec)',newline,'(c)'])
xlim([80 900])
ylim([0 0.15])
ylabel('SSTE (sec^2)')
legend([plot(Tbl(80001:end),SSE_Th_bl(80001:end),'g-.','LineWidth',2)
...
    plot(Tbl(80001:end),SSE_Th_bm(80001:end),'r-','LineWidth',1.5)],
...
    'Symmetric LBCM', 'Asymmetric LBCM');
title('T_{h,des} = 1.1 sec');
grid on
box on

set(findall(gcf,'-property','FontSize'),'FontSize',14);

%%%%%%%%%%%%%%%%%%%%%%%%%%%%%%%%%%%%%%%%%%%%%%%%%%%%%%%%%%%%%%%%%%%%%%%
%
```

```
% print('-dpng', '-r300', [plot_folder,'modelYZ']);



function [dy] = bmcarflw(t,y,N,Tfinal,Xfinal,Vfinal,kd_2,Th_const)

dy = zeros(2*N,1);

%---Model Parameters --BM
kd_1 = 1.9589;      %0.9717
kv = 0.32;         %0.4254
kc = 0.04;         %0.0028
l = 15;
T_headway = Th_const;

v_des = 31.44;
v_max = 33.528;

a_min = ones(N,1)*(-0.21*9.81);
min_gap = 5;
%%%%%%%%%%%%%%%%%%%%%%%

x0 = interp1(Tfinal,Xfinal,t);
v0  = interp1(Tfinal,Vfinal,t);

%%%%%%%%%%%%%%%%%%%%%%%
```

```
a_max = zeros(N,1);
p1 = 2.98e-06;
p2 = -5.69e-05;
p3 = -0.001084;
p4 = -3.059e-05;
p5 = 0.5547;

for i = 1:N
    speed = y(i+N);
    if speed>22.3
        a_max(i,1) = 0.1209052;
    else
        a_max(i,1) = p1*speed^4 + p2*speed^3 + p3*speed^2 + p4*speed +
p5;
    end
end

%-main system-- %%%%
for i=1:N
    dy(i) = y(i+N);
end

d_des = T_headway*y(N+N);
lead_gap = y(N-1)-y(N)-l;
```

```
if d_des<min_gap
    d_des = min_gap;
end

dy(N+N) = kd_1*(y(N-1) - y(N) - l - d_des) + kv*(y(2*N-1) - y(N+N)) ...
                +kc*(v_des - y(N+N));

if dy(N+N)>a_max(N,1)
    dy(N+N) = a_max(N,1);
elseif dy(N+N)<a_min(N,1)
    dy(N+N) = a_min(N,1);
end

if y(N+N)>=v_max && dy(N+N)>0
    dy(N+N) = 0;
end



for i = 1:N-1
    d_des = T_headway*y(i+N);

    if d_des<min_gap
        d_des = min_gap;
    end

    if i == 1
```

```
        lead_gap = x0 - y(i) - l;
        dy(i+N) = kd_1*(x0 - 2*y(i) + y(i+1)) + kd_2*(lead_gap-
d_des)...
                + kv*(v0 - 2*y(N+i) + y(N+i+1)) + kc*(v_des - y(N+i));
        if dy(i+N)>a_max(i,1)
            dy(i+N) = a_max(i,1);
        elseif dy(i+N)<a_min(i,1)
            dy(i+N) = a_min(i,1);
        end


        if y(i+N)>=v_max && dy(i+N)>0
            dy(i+N) = 0;
        end


    else
        lead_gap = y(i-1) - y(i) - l;
        dy(i+N) = kd_1*(y(i-1) - 2*y(i) + y(i+1)) + kd_2*(lead_gap-
d_des) ...
                      + kv*(y(i-1+N) - 2*y(i+N) + y(i+1+N)) ...
                       + kc*(v_des - y(N+i));
        if dy(i+N)>a_max(i,1)
            dy(i+N) = a_max(i,1);
        elseif dy(i+N)<a_min(i,1)
            dy(i+N) = a_min(i,1);
        end
```

```
        if y(i+N)>=v_max && dy(i+N)>0
            dy(i+N) = 0;
        end

    end

end

end


function [dy] = HornWang(t,y,N,Tfinal,Xfinal,Vfinal,kd_2,Th_const)

dy = zeros(2*N,1);

%---Model Parameters --BM
kv = 1.6170;
kd_1 = 0.8322;
kc = 9.927e-4;
l = 15;
T_headway = Th_const;



v_des = 31.44;
v_max = 33.528;
```

```
a_min = ones(N,1)*(-0.21*9.81);
min_gap = 5;
%%%%%%%%%%%%%%%%%%%%%%%

x0 = interp1(Tfinal,Xfinal,t);
v0  = interp1(Tfinal,Vfinal,t);

%%%%%%%%%%%%%%%%%%%%%%%

a_max = zeros(N,1);

p1 = 2.98e-06;
p2 = -5.69e-05;
p3 = -0.001084;
p4 = -3.059e-05;
p5 = 0.5547;

for i = 1:N
    speed = y(i+N);
    if speed>22.3
        a_max(i,1) = 0.1209052;
    else
        a_max(i,1) = p1*speed^4 + p2*speed^3 + p3*speed^2 + p4*speed +
p5;
    end
```

```
end

%-main system-- %%%%
for i=1:N
    dy(i) = y(i+N);
end

d_des = T_headway*y(N+N);
lead_gap = y(N-1)-y(N)-l;

if d_des<min_gap
    d_des = min_gap;
end

dy(N+N) = kd_1*(y(N-1) - y(N) - l - d_des) + kv*(y(2*N-1) - y(N+N)) ...
                +kc*(v_des - y(N+N));

if dy(N+N)>a_max(N,1)
    dy(N+N) = a_max(N,1);
elseif dy(N+N)<a_min(N,1)
    dy(N+N) = a_min(N,1);
end

if y(N+N)>=v_max && dy(N+N)>0
    dy(N+N) = 0;
end
```

```
for i = 1:N-1
    d_des = T_headway*y(i+N);

    if d_des<min_gap
        d_des = min_gap;
    end

    if i == 1
        lead_gap = x0 - y(i) - l;
        dy(i+N) = kd_1*(x0 - 2*y(i) + y(i+1)) + ...
                  kv*(v0 - 2*y(N+i) + y(N+i+1)) + kc*(v_des - y(N+i));
        if dy(i+N)>a_max(i,1)
            dy(i+N) = a_max(i,1);
        elseif dy(i+N)<a_min(i,1)
            dy(i+N) = a_min(i,1);
        end

        if y(i+N)>=v_max && dy(i+N)>0
            dy(i+N) = 0;
        end

    else
        lead_gap = y(i-1) - y(i) - l;
        dy(i+N) = kd_1*(y(i-1) - 2*y(i) + y(i+1)) +  ...
                     kv*(y(i-1+N) - 2*y(i+N) + y(i+1+N)) ...
```

```
                    + kc*(v_des - y(N+i));
        if dy(i+N)>a_max(i,1)
            dy(i+N) = a_max(i,1);
        elseif dy(i+N)<a_min(i,1)
            dy(i+N) = a_min(i,1);
        end

        if y(i+N)>=v_max && dy(i+N)>0
            dy(i+N) = 0;
        end

    end

end


end
```

REFERENCES

Arem, B. van, Driel, C.J.G. van, Visser, R., 2006. The Impact of Cooperative Adaptive Cruise Control on Traffic-Flow Characteristics. IEEE Transactions on Intelligent Transportation Systems 7, 429–436. https://doi.org/10.1109/TITS.2006.884615

Bhoopalam, A.K., Agatz, N., Zuidwijk, R., 2018. Planning of truck platoons: A literature review and directions for future research. Transportation Research Part B: Methodological 107, 212–228. https://doi.org/10.1016/j.trb.2017.10.016

Bonnet, C., Fritz, H., 2000. Fuel Consumption Reduction in a Platoon: Experimental Results with two Electronically Coupled Trucks at Close Spacing (SAE Technical Paper No. 2000- 01–3056). SAE International, Warrendale, PA. https://doi.org/10.4271/2000-01-3056

Bose, A., Ioannou, P., 2001. Analysis of Traffic Flow With Mixed Manual and Intelligent Cruise Control Vehicles: Theory and Experiments.

Chen, D., Laval, J., Zheng, Z., Ahn, S., 2012. A behavioral car-following model that captures traffic oscillations. Transportation Research Part B: Methodological 46, 744–761. https://doi.org/10.1016/j.trb.2012.01.009

Dey, K.C., Yan, L., Wang, X., Wang, Y., Shen, H., Chowdhury, M., Yu, L., Qiu, C., Soundararaj, V., 2016. A Review of Communication, Driver Characteristics, and Controls Aspects of Cooperative Adaptive Cruise Control

(CACC). IEEE Transactions on Intelligent Transportation Systems 17, 491–509. https://doi.org/10.1109/TITS.2015.2483063

Eyre, J., Yanakiev, D., Kanellakopoulos, I., 1998. A Simplified Framework for String Stability Analysis of Automated Vehicles. Vehicle System Dynamics 30, 375–405. https://doi.org/10.1080/00423119808969457

Freight and Congestion - FHWA Freight Management and Operations [WWW Document], 2017. URL https://ops.fhwa.dot.gov/freight/freight_analysis/freight_story/congestion.htm (accessed 7.5.21).

Geographic Area Series: Shipment Characteristics by Origin Geography by Mode: 2017 and 2012 [WWW Document], 2021. URL https://data.census.gov/cedsci/table?q=cf1700a01&hidePreview=true&tid=CFSAREA2017.CF1700A01 (accessed 7.5.21).

Gipps, P.G., 1981. A behavioural car-following model for computer simulation. Transportation Research Part B: Methodological 15, 105–111. https://doi.org/10.1016/0191-2615(81)90037-0

Goldberg, D.E., Holland, J.H., 1988. Genetic algorithms and machine learning.

Harwood, D.W., 2003. Review of truck characteristics as factors in roadway design. Transportation Research Board.

Holland, J.H., 1992. Adaptation in natural and artificial systems: an introductory analysis with applications to biology, control, and artificial intelligence. MIT press.

Horn, B.K.P., Wang, L., 2018. Wave Equation of Suppressed Traffic Flow Instabilities. IEEE Transactions on Intelligent Transportation Systems 19, 2955–2964. https://doi.org/10.1109/TITS.2017.2767595

Kesting, A., Treiber, M., Schönhof, M., Helbing, D., 2008. Adaptive cruise control design for active congestion avoidance. Transportation Research Part C: Emerging Technologies 16, 668–683. https://doi.org/10.1016/j.trc.2007.12.004

Kim, K.-O., Rilett, L.R., 2001. Genetic-algorithm based approach for calibrating microscopic simulation models, in: ITSC 2001. 2001 IEEE Intelligent Transportation Systems. Proceedings (Cat. No.01TH8585). Presented at the ITSC 2001. 2001 IEEE Intelligent Transportation Systems. Proceedings (Cat. No.01TH8585), pp. 698–704. https://doi.org/10.1109/ITSC.2001.948745

Kwon, J.-W., Chwa, D., 2014. Adaptive Bidirectional Platoon Control Using a Coupled Sliding Mode Control Method. IEEE Transactions on Intelligent Transportation Systems 15, 2040–2048. https://doi.org/10.1109/TITS.2014.2308535

Li, Y., Zhao, H., 2017. A car-following model for connected vehicles under the bidirectional-leader following topology, in: 2017 IEEE 20th International Conference on Intelligent Transportation Systems (ITSC). Presented

at the 2017 IEEE 20th International Conference on Intelligent Transportation Systems (ITSC), pp. 1–5. https://doi.org/10.1109/ITSC.2017.8317663

Ma, T., Abdulhai, B., 2002. Genetic Algorithm-Based Optimization Approach and Generic Tool for Calibrating Traffic Microscopic Simulation Parameters. Transportation Research Record 1800, 6–15. https://doi.org/10.3141/1800-02

Martinec, D., Herman, I., Šebek, M., 2014. Two-sided wave-absorbing control of a heterogenous vehicular platoon. IFAC Proceedings Volumes, 19th IFAC World Congress 47, 8091–8096. https://doi.org/10.3182/20140824-6-ZA-1003.01433

Nowakowski, C., Shladover, S.E., Lu, X.-Y., Thompson, D., Kailas, A., 2015. Cooperative Adaptive Cruise Control (CACC) for Truck Platooning: Operational Concept Alternatives.

Park, B. (Brian), Qi, H. (Maggie), 2005. Development and Evaluation of a Procedure for the Calibration of Simulation Models. Transportation Research Record 1934, 208–217. https://doi.org/10.1177/0361198105193400122

Pline, J.L., 1999. Traffic Engineering Handbook, 5th ed. Institute of Transportation Engineers, Washington, DC, USA.

Ploeg, J., Serrarens, A.F.A., Heijenk, G.J., 2011. Connect & Drive: design and evaluation of cooperative adaptive cruise control for congestion reduction. J. Mod. Transport. 19, 207–213. https://doi.org/10.1007/BF03325760

Pueboobpaphan, R., Van Arem, B., 2010. Driver and vehicle characteristics and platoon and traffic flow stability: Understanding the relationship for design and assessment of cooperative adaptive cruise control. Transportation Research Record 2189, 89–97. https://doi.org/10.3141/2189-10

Rahman, M., Chowdhury, M., Dey, K., Islam, M.R., Khan, T., 2017. Evaluation of Driver Car-Following Behavior Models for Cooperative Adaptive Cruise Control Systems. Transportation Research Record 2622, 84–95. https://doi.org/10.3141/2622-08

Rahman, M., Khan, S.M., Chowdhury, M., Huynh, N., Ogle, J., Dey, K., Bhavsar, P., 2015. Incident Command System Strategies for Incident Management on Freeways: A Simulation Analysis. Presented at the Transportation Research Board 94th Annual MeetingTransportation Research Board.

Ramezani, H., Shladover, S.E., Lu, X.-Y., Altan, O.D., 2018. Micro-Simulation of Truck Platooning with Cooperative Adaptive Cruise Control: Model Development and a Case Study. Transportation Research Record 2672, 55–65. https://doi.org/10.1177/0361198118793257

Sarker, A., Shen, H., Rahman, M., Chowdhury, M., Dey, K., Li, F., Wang, Y., Narman, H.S., 2020. A Review of Sensing and Communication, Human Factors, and Controller Aspects for Information-Aware Connected and Automated Vehicles. IEEE Transactions on Intelligent Transportation Systems 21, 7–29. https://doi.org/10.1109/TITS.2019.2892399

Schultz, G.G., Rilett, L.R., 2004. Analysis of Distribution and Calibration of Car-Following Sensitivity Parameters in Microscopic Traffic Simulation Models. Transportation Research Record 1876, 41–51. https://doi.org/10.3141/1876-05

Sugimachi, T., Fukao, T., Suzuki, Y., Kawashima, H., 2013. Development of Autonomous Platooning System for Heavy-duty Trucks. IFAC Proceedings Volumes, 7th IFAC Symposium on Advances in Automotive Control 46, 52–57. https://doi.org/10.3182/20130904-4-JP-2042.00127

Swaroop, D., Hedrick, J.K., Chien, C.C., Ioannou, P., 1994. A Comparison of Spacing and Headway Control Laws for Automatically Controlled Vehicles1. Vehicle System Dynamics 23, 597–625. https://doi.org/10.1080/00423119408969077

Tordeux, A., Lassarre, S., Roussignol, M., 2010. An adaptive time gap car-following model. Transportation Research Part B: Methodological 44, 1115–1131. https://doi.org/10.1016/j.trb.2009.12.018

Treiber, M., Kesting, A., 2013. Car-Following Models Based on Driving Strategies, in: Treiber, M., Kesting, A. (Eds.), Traffic Flow Dynamics: Data, Models and Simulation. Springer, Berlin, Heidelberg, pp. 181–204. https://doi.org/10.1007/978-3-642-32460-4_11

Treiber, M., Kesting, A., 2011. Evidence of Convective Instability in Congested Traffic Flow: A Systematic Empirical and Theoretical Investigation.

Procedia - Social and Behavioral Sciences 17, 683–701. https://doi.org/10.1016/j.sbspro.2011.04.539

Treiber, M., Kesting, A., Helbing, D., 2006. Delays, inaccuracies and anticipation in microscopic traffic models. Physica A: Statistical Mechanics and its Applications 360, 71–88. https://doi.org/10.1016/j.physa.2005.05.001

Tsugawa, S., Jeschke, S., Shladover, S.E., 2016. A Review of Truck Platooning Projects for Energy Savings. IEEE Transactions on Intelligent Vehicles 1, 68–77. https://doi.org/10.1109/TIV.2016.2577499

Wang, J., Rajamani, R., 2002. Adaptive cruise control system design and its impact on highway traffic flow, in: Proceedings of the 2002 American Control Conference (IEEE Cat. No.CH37301). pp. 3690–3695. https://doi.org/10.1109/ACC.2002.1024501

Wang, L., Horn, B.K.P., 2019. Multinode Bilateral Control Model. IEEE Transactions on Automatic Control 64, 4066–4078. https://doi.org/10.1109/TAC.2019.2891490

Wang, Y., Han, Z., 1998. Stability of an automated vehicle platoon, in: Proceedings of the 1998 American Control Conference. ACC (IEEE Cat. No.98CH36207). Presented at the Proceedings of the 1998 American Control Conference. ACC (IEEE Cat. No.98CH36207), pp. 950–954 vol.2. https://doi.org/10.1109/ACC.1998.703548

Williams, R.L., Lawrence, D.A., 2007. Linear state-space control systems. John Wiley & Sons.

Yang, G., Xu, H., Wang, Z., Tian, Z., 2016. Truck acceleration behavior study and acceleration lane length recommendations for metered on-ramps. International Journal of Transportation Science and Technology 5, 93–102. https://doi.org/10.1016/j.ijtst.2016.09.006

Zegers, J.C., Semsar-Kazerooni, E., Fusco, M., Ploeg, J., 2017. A multi-layer control approach to truck platooning: Platoon cohesion subject to dynamical limitations. Presented at the 2017 5th IEEE International Conference on Models and Technologies for Intelligent Transportation Systems (MT-ITS), pp. 128–133. https://doi.org/10.1109/MTITS.2017.8005652

Zhang, J., Ioannou, P., 2004. Control of Heavy-Duty Trucks: Environmental and Fuel Economy Considerations.